University of Illinois at Urbana-Champaign

ACRC

Air Conditioning and Refrigeration Center A National Science Foundation/University Cooperative Research Center

Applications and Control of Air Conditioning Systems Using Rapid Cycling to Modulate Capacity

M. J. Poort and C. W. Bullard

ACRC TR-238 May 2005

For additional information:

Air Conditioning and Refrigeration Center
University of Illinois
Mechanical & Industrial Engineering Dept.
1206 West Green Street
Urbana, IL 61801

(217) 333-3115

Prepared as part of ACRC Project #161
Applications and Control of Systems Using Rapid-Cycling to Modulate Capacity
C. W. Bullard and P. S. Hrnjak, Principal Investigators

The Air Conditioning and Refrigeration Center was founded in 1988 with a grant from the estate of Richard W. Kritzer, the founder of Peerless of America Inc. A State of Illinois Technology Challenge Grant helped build the laboratory facilities. The ACRC receives continuing support from the Richard W. Kritzer Endowment and the National Science Foundation. The following organizations have also become sponsors of the Center.

Arçelik A. S.
Behr GmbH and Co.
Carrier Corporation
Cerro Flow Products, Inc.
Copeland Corporation
Daikin Industries, Ltd.
Danfoss A/S
Delphi Thermal and Interior
Embraco S. A.
Ford Motor Company
Fujitsu General Limited
General Motors Corporation
Hill PHOENIX
Hydro Aluminum Adrian, Inc.
Ingersoll-Rand/Climate Control
Lennox International, Inc.
LG Electronics, Inc.
Manitowoc Ice, Inc.
Modine Manufacturing Co.
Novelis Global Technology Centre
Parker Hannifin Corporation
Peerless of America, Inc.
Samsung Electronics Co., Ltd.
Sanden Corporation
Sanyo Electric Co., Ltd.
Tecumseh Products Company
Trane
Visteon Automotive Systems
Wieland-Werke, AG
Wolverine Tube, Inc.

For additional information:

Air Conditioning & Refrigeration Center
Mechanical & Industrial Engineering Dept.
University of Illinois
1206 West Green Street
Urbana, IL 61801

217 333 3115

Abstract

Rapid cycling of the compressor can be used to modulate capacity as an alternative to variable speed a/c and refrigeration systems. This paper outlines design recommendations to optimize rapid cycling performance based on experimental results contrasting different heat exchangers and other components. Rapid cycling has inherent compressor lift penalties associated with larger mass flow rates relative to variable speed operation which need to be minimized. To design for optimal rapid cycling performance, it is also important to prevent dryout (superheating) in the evaporator during the off-cycle, a major penalty as cycles are lengthened. By reducing the number of starts per hour, through increasing cycle lengths, compressor performance and reliability can be improved, and efficiency increased by reducing the number of startup power spikes. To increase cycle lengths while minimizing penalties, the off cycle performance in the evaporator should be optimized. During the off cycle, two mechanisms contribute to off cycle cooling: additional boiling of refrigerant, and warming of the evaporator thermal mass.

Experiments were done on a typical 2-ton residential system with a round tube and plate fin evaporator and compared to a similar 1-ton system with a microchannel evaporator to explore the tradeoffs in evaporator design. Other components including a receiver and a suction line heat exchanger were also tested. Evaporator design should be focused on preventing dryout by increasing the refrigerant side area and preventing off cycle drainage. Since the condenser does not have the dryout problem, its only design changes would be to add thermal mass if economically feasible. For optimal performance under rapid cycling conditions, it was found that it would be best to combine flash gas bypass with a suction line heat exchanger to maximize performance during the off cycle and increase cycle lengths without incurring major penalties. This would allow the careful control of refrigerant boiling during the off cycle and maximize the thermal mass contribution to cooling the air during the off cycle.

Table of Contents

List of Figures

Page

List of Tables

Page

Chapter1: Introduction

Air conditioning systems are usually designed to run at only one operating condition. In practice, however, energy can be saved by using variable speed systems to modulate the capacity. Rapid on-off cycling of a single-speed compressor could theoretically achieve results similar to variable speed systems, while avoiding the electrical cost and losses associated with inverters. The goal of this project was to establish general guidelines for optimizing the overall design and compressor selection for rapid cycling systems. The internal design of the compressors is not addressed here, because the design of the rest of the system is independent of the compressor details.

In rapid cycling the compressor is turned on & off in repeated cycles shorter than ~70 seconds. Capacity modulation is regulated by controlling the fraction of the cycle length during which the compressor is on. Since the cycles are short, the pressure lift oscillates around a mean that is close to that of variable speed operation. Figure 1.1 shows schematically the saturation temperatures on the high and low side of the system and the temperature lifts for each operating condition.

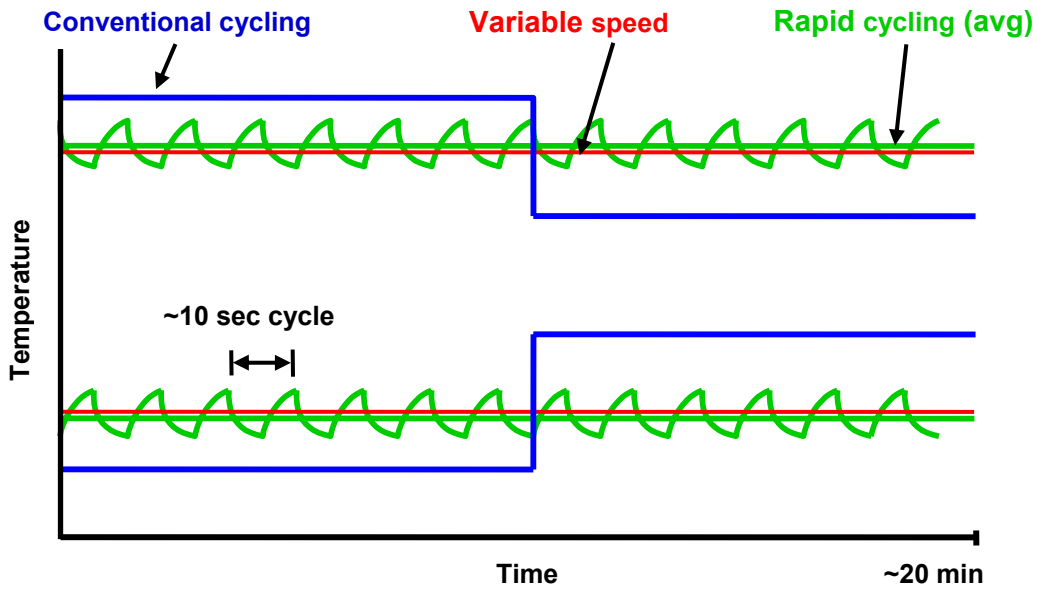

Figure 1.1 Diagram of temperature lift for different types of operation.

Lower on-cycle temperature lift requires less compressor work for the same mass flow. In rapid cycling, when cycles are stretched out long enough, performance approaches that of conventional (long) cycling. On the other hand, when cycles are extremely short, performance approaches that of a variable speed system. For reasons of compressor reliability it is desirable for cycles to be stretched as long as possible without deviating too far from the temperature lift associated with variable speed operation.

Experiments by Ilic et al. (2001), demonstrated that on-off cycling of the compressor can achieve efficiencies within 2.5% of a variable speed system's cycle COP. These experiments also revealed that there was almost no off-cycle boiling so all the pressure drop and refrigerant-side temperature difference occurred during the on cycle. For a 50% capacity case this meant that the refrigerant temperature difference and pressure drop were about twice as large during the on cycle. During the off cycle, cooling continued as heat was transferred from the air

to the thermal mass of the evaporator, but off-cycle dryout (superheating) in sections of the evaporator degraded performance significantly during the longer cycle periods. Ilic identified the loss mechanisms unique to rapid cycling as the pressure drop, refrigerant temperature difference and nonlinearity penalties. The pressure drop and refrigerant temperature difference loss terms stem from the need to pass twice as much refrigerant through the heat exchangers in half the time. The nonlinearity penalty refers to the differences between the on-cycle and whole-cycle average temperatures of the heat exchangers, these asymmetrical oscillations are especially noticeable in heat exchangers having low thermal capacitance.

Experiments also indicated that it was be best to isolate the high and low side of the system using two solenoid valves to maintain the saturation pressures on both sides of the system during the off cycle. Ilic et al concentrated primarily on lengthening cycles by increasing the thermal capacitance of the heat exchangers in order to achieve temperature oscillations that remained nearly symmetrical over longer cycle periods, thus minimizing degradation of temperature lift associated with the exponential nature of heat transfer. The performance margin (2.5 % of variable speed system COP) is smaller than the inverter losses that would further degrade variable speed system COP. This paper describes subsequent experiments designed to explore the potential for further optimization of the overall system.

Due to the high cost of increasing the evaporator and condenser thermal mass, and the difficulty of avoiding evaporator dryout during longer off cycles, a different approach was taken, involving installation of a microchannel evaporator in the same facility used by Ilic. Due to the greater refrigerant side area; an appropriately designed microchannel evaporator would have a smaller refrigerant-side temperature difference, and a smaller pressure drop due to the large number of multi-port tubes. Thus minimizing these variables and their associated temperature lift penalties in the variable-speed baseline case makes the evaporator less vulnerable to the losses incurred when these parameters increase during rapid cycling. Unfortunately the best-available prototype microchannel heat exchanger was far from an ideal evaporator prototype because it had been designed as a CO_2 gas cooler and therefore had ports that were too small and too little in number for our R22 system. Nevertheless it did prove adequate for testing hypotheses about the nature and magnitude of the loss mechanisms inherent in rapid cycling systems. Since the evaporator was still vulnerable to dryout, experiments remained focused on shorter cycle periods (5-20 seconds). Experimental results are summarized below, and followed by overall system design recommendations based on the comparison with results obtained using conventional heat exchangers and different arrangement of other components. For full details see the appendices.

Chapter 2: Apparatus and methods

The experimental setup consisted of a residential split system installed in an instrumented outdoor and indoor chamber. Previous work was done on heat exchangers from a two-ton, R-22 unitary rooftop air conditioning system (Trane TCH024100A) with a two-ton hermetic scroll compressor (Copeland model ZR22K3-TF5) as described by Ilic et al. The TXV was replaced by an electronic expansion valve which allowed more precise control while avoiding the inherent lag of a TXV which is problematic without a steady mass flow. The microchannel evaporator, suction line heat exchanger and 1 ton reciprocating compressor (Copeland model KAN 0075) were later installed by Uribe et al. (2003). Other changes made to the experimental setup primarily concerned the location of measurements and are further detailed in appendix A.

All temperatures were measured by T-type thermocouples and probes that were calibrated initially between an ice bath and room temperature, and again prior to each set of experiments by adjusting tare values at room temperature. The uncertainty of thermocouple measurements was estimated to be ± 0.1°C. To measure air flow rate, a 0-1" water differential air pressure transducer was used to detect the pressure drop across the nozzle with an error of ± 0.4 % of full scale. The absolute pressures were measured at the evaporator and compressor outlets with ±0.5 psia error. Pressure differences were also detected across both heat exchangers with ±0.125 psid error. Refrigerant mass flow was measured using a Coriolis type mass flow meter within ±0.15% error. The power to the compressor, blower and heaters were measured using watt transducers with ±40 W error. Data from each experiment was obtained after the rapid-cycling system reached an equilibrium operating state characterized by stable repeatable cycles. All calculations were performed using 200-second averages of data recorded at 0.2 second intervals. The data plots for single cycles show a typical cycle selected from the 200-second record.

Chapter 3: Evaporator performance

Evaporator temperatures and pressure were recorded during steady repeatable oscillations at rapid cycling conditions that could be compared to variable speed operation at the same cooling capacity. As cycle periods got shorter, the amplitude of oscillations diminished until the mean values of all thermodynamic variables approached those of variable speed operation.

Refrigerant pressure drop across the evaporator was one of these oscillating measurements that displayed behavior important to understanding rapid cycling. While the magnitude of this pressure drop would have been lower with an optimally designed evaporator, its behavior yielded qualitative insights. Significant on-cycle pressure drop was not reached for about two seconds while the liquid inventory was being re-established during the on cycle, and it continued to rise as the saturation temperature declined and more boiling occurred in the evaporator. After compressor shut down 8 seconds into the cycle, the pressure drop reveals that boiling continued for about 4 more seconds as the remaining liquid evaporated. Figure 3.1 shows the whole-cycle pressure drop to be significantly higher than that measured during variable speed operation.

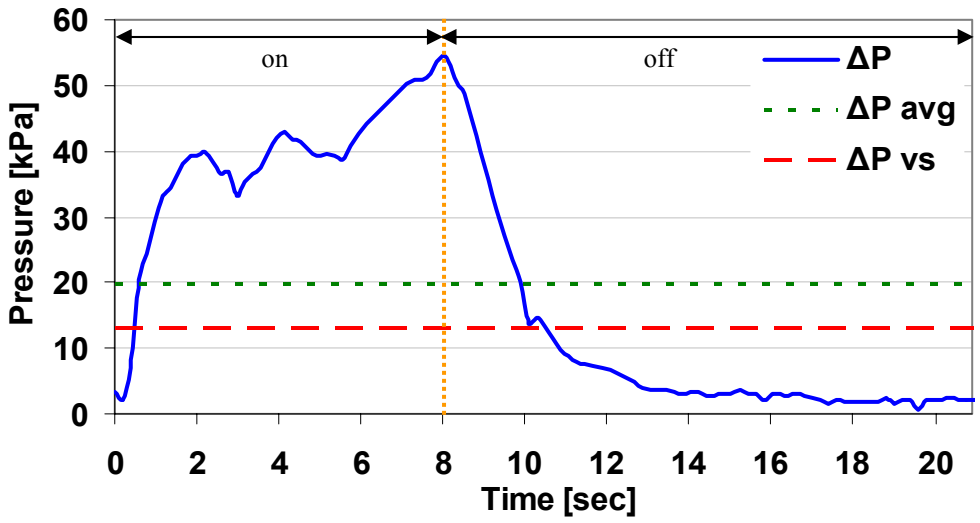

Figure 3.1 Evaporator pressure drop 0.4 runtime fraction, ~20 second cycle.

In shorter cycles such as the 5 second cycle in Figure 3.2, the pressure drop did not have a chance to establish itself during the on cycle. It is also likely that the walls never dried out since there is not enough time to boil all the liquid from the evaporator. Due to the short cycle length, the whole-cycle average pressure drop is much closer to that of variable speed operation, even though the compressor was only on during the first two seconds of the cycle. Thermodynamic performance of even shorter cycles would approach that of variable speed systems more closely.

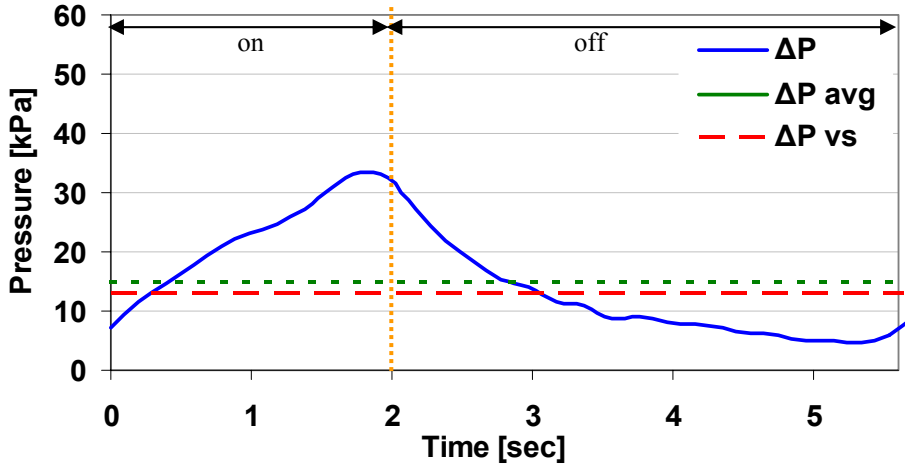

Figure 3.2 Evaporator pressure drop 0.4 runtime fraction, ~5 second cycle.

Repeatable oscillations also occurred in most temperatures recorded throughout the experimental setup. Figure 3.4 shows the temperatures on the low side of the system for a ~20 second cycle while Figure 3.3 indicates the locations of these measurements around the evaporator. In these longer cycles dryout and superheating occurred in the evaporator tubes. This was shown by the temporary deviation during the on cycle of the immersion thermocouple from the saturation temperature at the evaporator exit. This superheat 'bubble' occurred when there was enough boiling during the off cycle that large areas of the evaporator dried out and superheated. During the next on cycle it took a few seconds for this superheated region to be pushed through the evaporator as the liquid inventory was re-established.

Note the cross-parallel flow configuration of the evaporator is shown in Figure 3.3 with its 3 rows of vertical flat multi-port tubes forming uninterrupted parallel circuits between the inlet and outlet header. This prototype was selected because it had no intermediate headers that could have exacerbated refrigerant maldistribution and introduced measurement uncertainties.

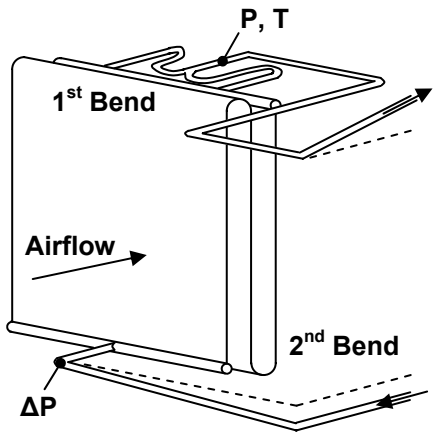

Figure 3.3 Evaporator instrumentation.

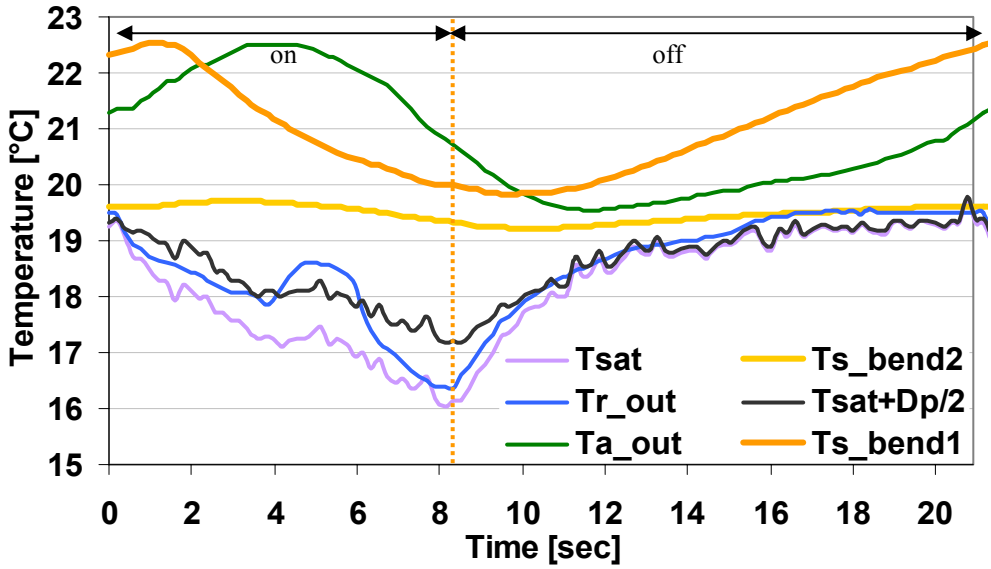

Figure 3.4 Evaporator refrigerant, metal, and air temperatures for a 40 %, ~20 second cycle.

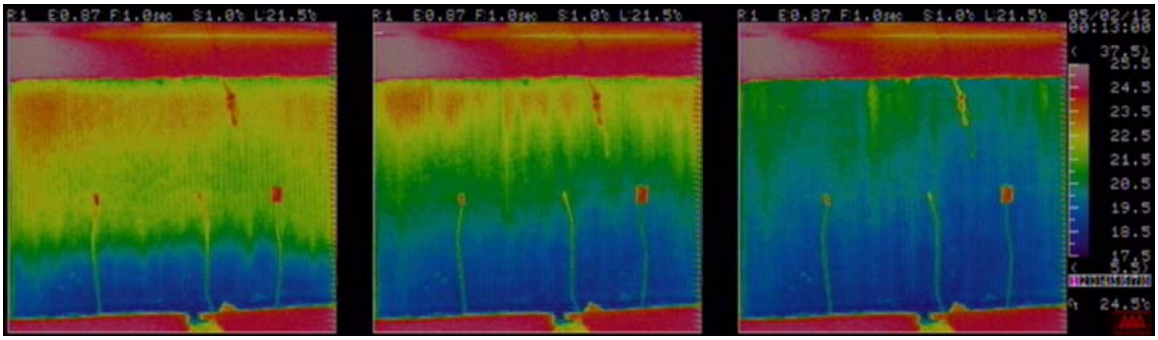

Figure 3.5 Infrared picture sequence of the first two seconds of the front slab of the evaporator of a 20 second 40% cycle.

Metal temperatures continued to rise a few seconds after the start of the on cycle due to the delay associated with re-establishment of the liquid inventory. Because the evaporator had dried out during the off cycle, the liquid front moved slowly through the evaporator bringing the metal temperature back down to saturation temperature during the next on-cycle. Tube surface temperatures in the first bend of the evaporator did not begin to decrease until ~1.5 seconds, when the liquid front re-wetted that area of the evaporator. Figure 3.5 shows the liquid front moving through the front slab of the evaporator during the first two seconds of an 8-second on cycle. The temperature of the second (bottom) bend of the evaporator tubes had risen more slowly during the off cycle than the first bend, because it received air already cooled by the first slab and liquid draining downwards from the tubes in the second and third slabs. About 1 second after the liquid front moved through the first bend, the liquid front then moved through the second bend. It took slightly less time to re-establish the liquid inventory in the second slab than the first because it was less heavily loaded and its on-cycle liquid inventory was smaller.

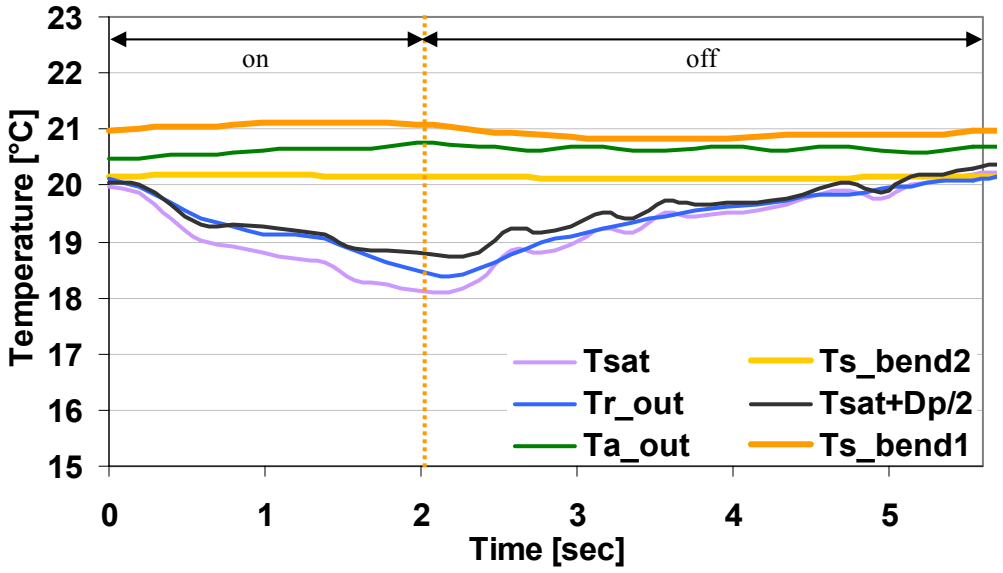

Figure 3.6 Evaporator refrigerant, metal, and air temperatures for a 40 %, ~5 second cycle.

Figure 3.6 shows how cycles of ~5 seconds exhibited virtually no oscillation in metal and air temperatures. Recall from Figure 3.2 that pressure drop remained positive throughout the off cycle, indicating that the refrigerant flow and evaporation continued throughout. The temperature profiles in Figure 3.2 confirm that the evaporator remained saturated without a chance for dryout to occur. While the compressor was only on for the first two seconds, the evaporator surface and air temperatures were nearly identical to variable speed operation. Saturation temperature did oscillate, rising during the off cycle as boiling maintained the small temperature difference between the refrigerant and the metal surface that was being heated by the air. During the on cycle the saturation temperature was pulled back down, re-establishing the liquid inventory in the evaporator. These oscillations were almost linear, so the evaporator and off-cycle refrigerant-side ΔT's were nearly equal (0.2°C difference in Figure 3.6). Similarly the on-cycle saturation temperature drop indicated in Figure 3.4 was only 0.4°C greater than the steady state case. This indicates that there were virtually no thermodynamic losses compared to variable speed operation.

The pressure drop, refrigerant temperature difference and nonlinearity temperature lift loss mechanisms identified by Ilic played a diminished role in shorter cycles. The temperature lift penalty due to non-linearity was non existent due to regular, linear oscillations. The pressure drop penalty was drastically reduced because its steady state values were not attained within short on cycles such as the ~5 second cycle in Figure 3.2. In this operating condition the magnitude of the pressure drop penalty was only 30% during the on cycle due to the pressure drop (boiling) that occurs while the compressor is off. In these short cycles the refrigerant temperature difference was also spread between the on and off cycles. Since the lift penalty is only paid during the on cycle, the refrigerant temperature difference was only about 60% of that observed during full speed operation. These differences in shorter cycles allow performance to approach that of variable speed systems.

Chapter 4: Evaporator design implications

Optimal design for rapid cycling primarily consists of stretching out cycle lengths, maintaining significant off-cycle cooling while avoiding penalties associated with long off cycles. Our motivation in lengthening off cycles was to reduce the number of compressor starts, recognizing that fewer power spikes (which are partly dissipative) increase performance and reliability of the compressor. While data showed significant energy contained in the power spikes for short cycles due to the use of a relay to turn the compressor on and off, it is possible that simple electronics may have the capacity to reduce their magnitude at a cost far less than that of an inverter drive. An existing commercial application of the rapid-cycling technology, Copeland's Digital Scroll, disengages the scroll and idles the motor, incurring a power penalty and heating the suction gas during the off-cycle. Compressor selection would be driven by such tradeoffs between reliability and efficiency, after designing other components to maximize cycle length.

Particularly valuable insights into rapid cycling penalties were gained by comparing measurements from the conventional copper tube and aluminum fin evaporator to the microchannel prototype. Figures 4.1 and 4.2 contrast the temperature profiles during ~10 second cycles for the two evaporators.

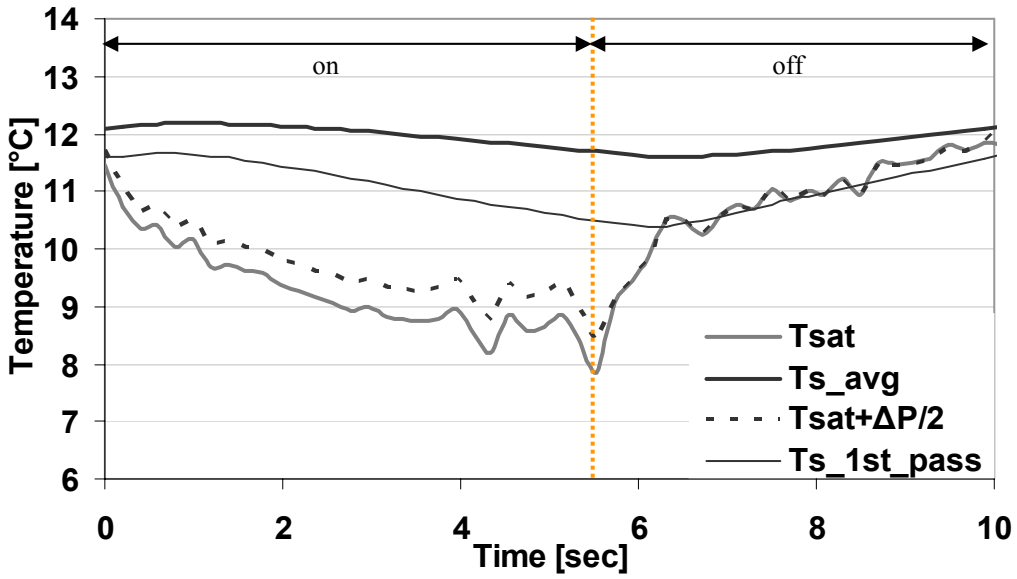

Figure 4.1 Round tube and plate fin evaporator temperatures, 10 sec 56% capacity.

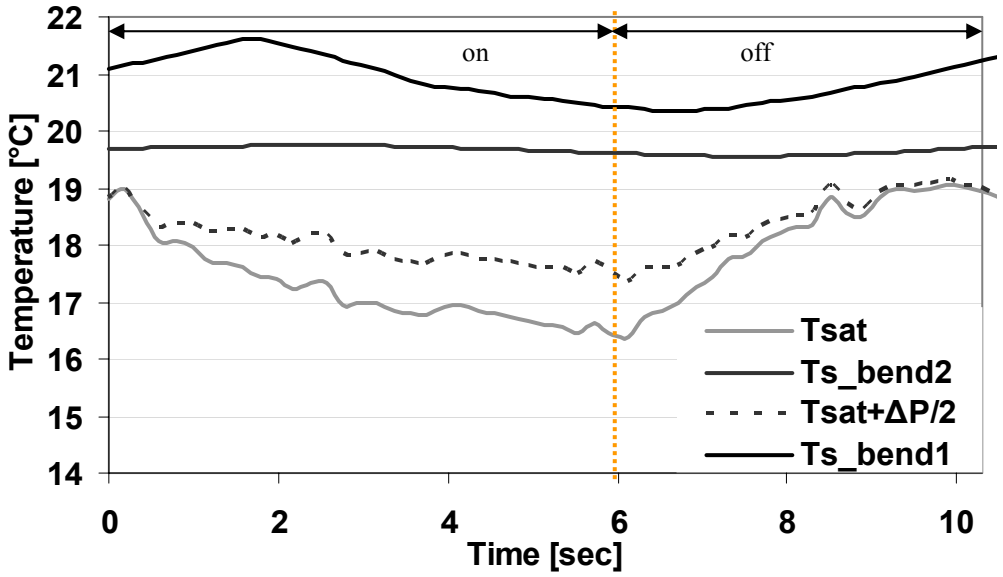

Figure 4.2 Microchannel evaporator temperatures, 10.3 sec 0.58 capacity fraction.

Two mechanisms cool air during the off cycle, the boiling of liquid refrigerant in the evaporator and the warming of the thermal mass of the tubes and fins. In the conventional round tube/plate fin experiments (Figure 4.1) there was little off-cycle boiling in the evaporator, due to the limited volume on the low side of the system. While there was a large liquid inventory in the evaporator at compressor shutdown, the saturation temperature rose quickly to the metal temperature, preventing further boiling. The majority of the off-cycle cooling was done as the thermally massive evaporator (and its saturated refrigerant inventory) slowly warmed up.

In the microchannel evaporator, there was less thermal capacitance and more wetted surface area to allow more evaporation before dryout. While the total low side volume (including the large high-effectiveness suction line heat exchanger) was virtually the same as in the conventional system, the suction line heat exchanger provided a cold area for refrigerant to condense during the off cycle. Instead of the saturation pressure rising due to boiling in the evaporator, the liquid side of the suction line heat exchanger with its heavily insulated and thermally massive tubing and liquid refrigerant mass maintained a cold zone where condensation took place. The condensation allowed the refrigerant to continue boiling in the evaporator (cooling the air) without immediately raising the saturation temperature. Therefore the saturation temperature rose slowly, maintaining a finite temperature difference between the metal and refrigerant, instead of the saturation temperature and pressure rising immediately as it did in the round tube-plate fin evaporator. The heat of condensation released on the low side of the suction line heat exchanger only marginally affected sub-cooling (and therefore performance) at the beginning of the next on cycle since only 10 g could have condensed, and the suction line heat exchanger thermal mass was large enough to absorb that energy without increasing the temperature of the refrigerant in the liquid line.

The primary factor limiting rapid-cycling performance is dryout of the evaporator walls. When dryout occurs, the refrigerant and metal surface temperatures rise above the saturation temperature, reducing the air-to-surface temperature difference and reducing the cooling that can occur. During the next on cycle flash boiling occurs

and it takes several seconds for the metal temperatures to be reduced enough to re-establish boiling throughout the evaporator.

A number of things can be done to lengthen cycle periods by delaying dryout in the evaporator. One option would be to limit low side volume of the system to ensure that boiling stops before dryout occurs similar to the experiments with the round tube and plate fin evaporator. This would shift the off cycle cooling mechanism from boiling to reliance on the evaporator thermal mass to stretch out the off cycle. However, our experiments demonstrated that this strategy is ineffective if the low side temperature is not uniform and isothermal. While the temperatures were equal when all surface was wetted, dryout occurred as refrigerant vaporized and it was accelerated by liquid drainage from the evaporator tubes during the off cycle. Once dryout started, a heat pipe effect within the evaporator further contributed to superheating of the evaporator tubes. As vapor was superheated, the cooler wet regions caused the vapor to condense, in turn causing additional dryout as more refrigerant vaporized from the regions where the refrigerant film was thinnest.

The second approach to suppress dryout is to increase the amount of wetted refrigerant side area in the evaporator, increasing the amount of refrigerant on the walls of the evaporator tubes. This would increase the amount of refrigerant available for boiling and therefore extend the time it takes for a given average film thickness of refrigerant to evaporate. Other ways to reduce dryout in the evaporator would focus on getting better distribution and more liquid refrigerant into the evaporator. The ideal situation would be for the liquid film to be distributed in such a way that when dryout does occur it happens on all evaporator surfaces at once.

Chapter 5: Condenser design

As in the case of variable speed systems, the condenser is the main source of energy savings in rapid cycling systems. The evaporator's contribution to reducing lift is limited by the need to dehumidify, and its performance can be impaired by dryout during long off cycles. During rapid cycling the condenser displays many of the same but opposite behaviors as the evaporator. In the condenser the film thickness buildup on the tube walls increases heat transfer resistance during the off cycle, but has an insignificant effect on system performance. The condenser would be sized for the maximum capacity condition, the same as a variable speed system (optimal fan speed control would be equally effective in each case). Tube diameters and circuiting, however, would be optimized for the heat transfer and pressure drop tradeoff at a single compressor speed instead of ranging over a factor of [say] five. Finally a condenser optimized for rapid cycling would have sufficient thermal mass to suppress non-linear surface temperature oscillations over the cycle length a period constrained by the onset of dryout in the system's evaporator.

Chapter 6: Other components

In design for rapid cycling systems careful consideration must be given to other components that could enhance performance on the low side of the system. A high side receiver in combination with a high effectiveness suction line heat exchanger used in the microchannel experiments was best possible setup in our lab, given the space constraints. This setup ensured superheating at the compressor inlet, saturated refrigerant at the evaporator outlet and pure liquid at the expansion valve.

In practice a better alternative would be to use a flash gas bypass in combination with a medium effectiveness heat exchanger (Figure 6.1). During the on cycle, this would ensure good refrigerant distribution by allowing single phase liquid to enter the evaporator. At the same time the suction line heat exchanger would ensure a saturated condition the evaporator outlet, so each off cycle would begin with a thicker refrigerant film on the tube walls and larger liquid inventory. The bypass valve would adjust to create the same pressure drop as the evaporator, maintaining the desired liquid level in the flash tank. The level could be adjusted to control the condenser outlet state. The suction line heat exchanger would superheat the vapor with the expansion valve controlling the level of superheat. Since the suction line heat effectiveness was too high (larger than ~97 % in our experiments) the resulting cold spot at its liquid outlet exacerbated the evaporator dryout problem by providing a location cold enough for refrigerant to condense. A larger temperature difference across a smaller suction line heat exchanger would maintain its metal temperature above the low side saturation temperature, preventing condensation during the off cycle.

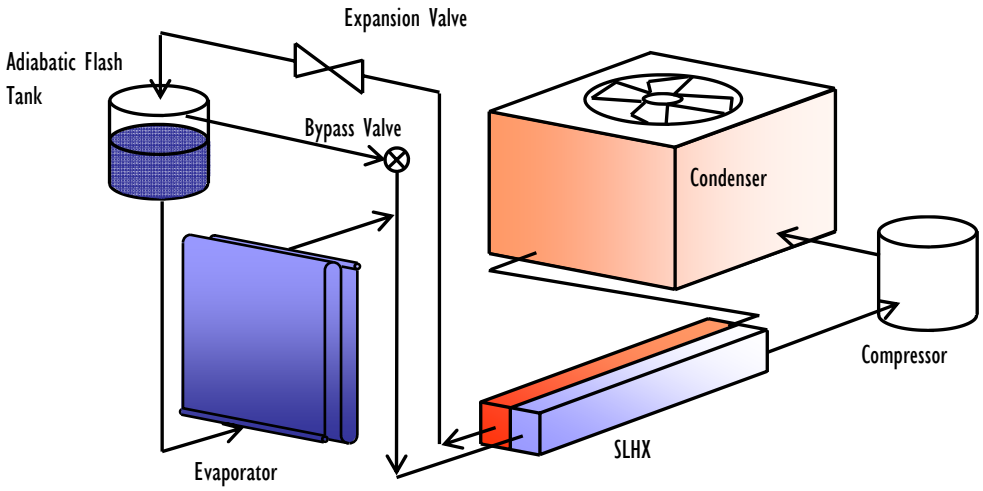

Figure 6**Error! No text of specified style in document.**.1 Diagram of the component setup for rapid cycling.

At the start of the off cycle, solenoid valves isolate the low side from the expansion valve to the compressor to maintain the high and low side pressures as described by Ilic et al. The saturation temperature would therefore rise as liquid boiled in the evaporator. The potential energy of the refrigerant in the flash tank (located above the bottom of the evaporator) would allow additional liquid refrigerant to seep into the evaporator. A typical low side vapor volume would allow boiling of ~5 g before the 3°C refrigerant temperature difference between the metal and refrigerant would be reduced to zero. Additionally, the liquid in the flash tank provides a cold area for vapor to

condense similar to what happened in the suction line heat exchanger in previous experiments. However this condensation is limited by the refrigerant mass in the flash tank. The condensation would continue until the temperature of all the low side refrigerant was raised to the metal temperature. This condensation would allow a controlled amount of boiling of ~10g out of the evaporator for every 500g of liquid refrigerant in the low side to rise 3°C. Thus the refrigerant-to-metal temperature difference in the evaporator would be reduced to zero by the evaporation of only ~15 g of refrigerant. If the evaporator tube walls held significantly more than ~15 g of liquid, and/or the evaporator was partially replenished with liquid draining from the flash tank, the dominant off-cycle cooling mechanism would result from warming the thermal mass of the evaporator and its refrigerant. During the next on-cycle the compressor would reduce the saturation temperature and the flooded evaporator would gradually start returning to steady state operation. To ensure proper performance, the flash tank should be located near the top of evaporator and the plumbing should include a trap to prevent liquid from seeping into the suction line heat exchanger during the off cycle.

One of the drawbacks of this type of system is the cost of the additional valve which will have to be adjusted for different operating conditions to balance the pressure drop through the evaporator. Dynamic control of this additional valve is required to adjust for different operating conditions and perhaps to control flow during cycling transients. The absence of a high side receiver also requires careful management of charge in the flash tank to prevent flooding or starving in the condenser.

To stretch out off cycles even more, the thermal mass of both heat exchangers would have to be increased. While adding metal mass to the evaporator and condenser would be very costly it is possible to locate the thermal mass outside of the heat exchangers using secondary water loops such as found in a chiller. A brazed plate heat exchanger would cool the water during rapid cycling operation, while the air coil would be utilized 100% of the time. Water could be stored in tanks or within a large shell and tube heat exchanger to provide a large heat sink. From a performance standpoint the additional ~5% pumping power and lift penalty due to a second heat exchanger in each loop would introduce more losses than the benefits provided by the additional thermal mass. In the analysis presented in Appendix F, it was evident that the extra costs of the water loop for the cycling chiller, and its inherent inefficiency, means that it is not an effective way to increase the thermal mass in the rapid cycling system.

The sizing of a rapid cycling system would be done in similar fashion to variable speed systems, where appropriate capacity and operating conditions were chosen for an application. Most of the rapid cycling design would be done on the low side as the only differences on the high side would be an economically feasible increase of the thermal mass relative to that of a variable speed condenser. The evaporator would be designed to prevent dryout by creating a large amount of refrigerant side area relative to the air side area. To increase refrigerant side area, ports would be thinner and more numerous. There would be a larger liquid refrigerant inventory spread out over more tube surface area. The amount of boiling desired during the off cycle would be controlled by the low side volume and the liquid level in the flash tank. The suction line heat exchanger would be designed so that it is as effective as possible without creating a cold area that would allow off-cycle condensation. The thermal capacitance of the condenser would have to be increased according to that of the evaporator; it must be large enough to keep

refrigerant oscillations nearly linear (i.e. on-cycle average ≈ whole-cycle average) but doesn't have the dryout problem.

Runtime fraction would be determined by the load, and off cycle duration would be as long as possible without incurring a dryout penalty. One method to achieve this would be to restart the compressor when superheat is detected in the warmest part of the evaporator. To decrease the likelihood of dryout occurring in the evaporator, a variety of piping and circuiting arrangements could feed liquid into the evaporator in a manner that keeps all the tube surfaces wetted.

Chapter 7: Conclusions

Rapid cycling can provide performance comparable to variable speed systems without incurring the cost of an inverter. The question of feasibility is therefore an economic one. To maximize performance and make rapid cycling feasible it is important to stretch out cycle lengths as long as possible without degrading evaporator performance. Increasing cycle lengths improves compressor reliability and reduces the effect of dissipative startup power spikes. Experimental results show that at very short (~5 second) cycles air and metal temperatures are nearly constant, so heat exchanger performance is similar to variable speed operation. To extend cycle lengths, off cycle duration is the limiting factor, for eventually heat exchanger surface temperature oscillations become nonlinear and dryout occurs. Off-cycle cooling occurs either through the warming of the thermal mass or due to the boiling of refrigerant left in the evaporator at the end of the on cycle.

To design for rapid cycling, cycle lengths can be maximized by increasing evaporator thermal mass and the amount of off cycle boiling, while preventing dryout from occurring in the evaporator. It would be best to use a flash gas bypass in combination with a suction line heat exchanger to increase the evaporator liquid inventory and maximize the use of the evaporator area by keeping it saturated throughout the off cycle. During the off cycle the thermal mass of the liquid in the flash tank limits the boiling that occurs in the evaporator before the saturation temperature reaches the metal temperature. Additional lengthening of off cycles can be accomplished by adding evaporator thermal mass.

References

Ilic, S. M., Bullard, C. W. and Hrnjak, P. 2001. Effect of short cycling compressor modulation on refrigeration system performance. ACRC CR-43.

Uribe, T., Bullard, C.W. and Hrnjak, P. 2003. Designing and optimizing systems for compressor rapid cycling. ACRC TR-220.

Incropera, F. P. and D. P. DeWitt, 1996. Fundamentals of Heat and Mass Transfer, John Wiley and Sons, New York, NY.

Stoecker W. F and Jones J. W. 1982. Refrigeration and air conditioning. Second edition. McGraw Hill, New York.

Kirkwood, A.C. and Bullard C.W. 1999. Modeling, design, and testing of a microchannel split-system air conditioner. ACRC TR-149.

Souza, A. and M. Pimenta, 1995. "Prediction of pressure drop during horizontal two-phase flow of pure and mixed refrigerants", In: J. Katz and Y. Matsumoto, editors. *Cavitation and Multiphase flow*, New York, NY: ASME, FED-Vol. 219, pp.161-171.

Wattelet, J. P., et al. 1994. Heat Transfer Flow Regimes of Refrigerants in a Horizontal-Tube Evaporator. ACRC TR-55.

Appendix A: Experimental Setup Changes

The experimental setup was originally constructed by Ilic et al. 2001 and modified Uribe et al. 2003, who installed the microchannel evaporator and high-effectiveness suction line heat exchanger. This appendix details the changes made in the experimental setup.

Changes of the actual experimental setup consisted primarily of more effective plumbing and new thermocouples on the low side. The evaporator configuration was changed by putting it in cross parallel flow so that the coldest refrigerant met the warmest air. The tubes between the expansion valve and the evaporator were changed from 3/8 to 1/4 inch diameter to reduce the refrigerant travel times to the evaporator inlet. The conventional evaporator that was located downwind of the microchannel (and before the nozzle air temperature measurement) was also removed because its thermal capacitance was interfering with measurements of downstream air flow. A thermocouple grid that detected horizontal air outlet temperature differences was installed (as opposed to vertical to determine distribution in the conventional evaporator). An additional thermocouple was also placed in the nozzle to confirm ΔT_{air} measurements. Some small changes were also made to accommodate additional (not related) experiments on a special suction line heat exchanger made of a sandwich of microchannel tubes.

On the high side compressors were changed but then changed back and there were only minor plumbing differences in the end. Thermocouples were also shifted around for more accurate measurement of refrigerant outlet and air and metal temperatures on the condenser.

Appendix B: Test matrix and data analysis method

The test matrix and data collection method was originally developed described by Ilic et al. 2001 and further expanded on by Uribe et al. 2003. This appendix details the subsequent changes in test matrix and data analysis with a specific focus on how measurements and cycles are averaged.

B.1 Test Matrix

The test matrix was changed slightly to make data more comparable. Our goal in this project was to make conclusions regarding optimization for rapid cycling systems. The most important part in setting up the test matrix was to find a good method to compare different data sets. It was determined that the best way to do this was to keep capacity constant when comparing rapid cycling to variable speed operation. There are numerous ways to keep the capacity constant in the laboratory. Since there was too much uncertainty in the metal temperature measurements in the evaporator (used in previous experiments) it was better use the air side energy equation and change the mass flow rate of the refrigerant at a set air flow rate to adjust capacity.

The first set of data was for full speed operation to establish a benchmark with a maximum Q_{evap}. The maximum refrigerant mass flow rate was used with an evaporator air flow rate (~800 cfm/ton) appropriate for the sizes of the compressor and the prototype evaporator. The air exit temperature was noted and then held constant throughout all the other experiments. This ensured a constant temperature difference since the inlet air was also constant. To experiment with different capacities, new air flow rates such as 40% were selected, and blower speed was reduced by the same percentage. The refrigerant mass flow rate was also adjusted to about 40% by altering the off-cycle time to retain the same cycle-average air side temperature difference. Short cycle lengths were also optimized in this manner by repeating the experiment with different on-times. This strategy was repeated for 60% and 80% operation to allow for some comparability to old data. Cycle lengths that were tested were 5, 10, 15 and 20 seconds, as previous data indicated that optimum cycle lengths lie within that range and dryout significantly degrades performance at cycles longer than 20 seconds. In addition to single cycle analysis, care was taken to create reliable ~200 second averages of the data to demonstrate repeatability and give a better indication of overall performance.

B.2 Averaging ΔT_{air}

When controlling experiments, it was important to keep Q constant so that the capacities exactly known and comparable. To keep Q_{cycle} constant, ΔT_{air} had to be kept constant in the lab. It was found that there were significant oscillations in longer cycles. To counter these oscillations, HPvee was used to calculate a real time "box car average" which averaged a variable set of the most recent readings. There was a slight problem that the readings do not occur regularly (due to slow computer) and it is therefore tough to define an appropriate moving average. However with the focus on ~200 second averages, this inaccuracy becomes negligible. When a data gets recorded this is not an issue as readings are written to a file at exact, ~0.2 second intervals.

B.3 Averaging Evaporator Metal Temperatures

One of the important variables needed to draw conclusions about evaporator performance was the metal temperature. There were a lot of differences in the metal temperatures of the evaporator at different locations

because of maldistribution and evaporator dryout. There are thermocouples epoxied to the micro channel tubes distributed throughout the evaporator. The thermocouples can only be placed on the two bends and the inlet and outlet headers. Originally more thermocouples were placed towards the high-quality region of the evaporator to get more insight when the most maldistribution is expected. Figure B.3.1 shows the geometry of the evaporator and a schematic with the locations of the numbered thermocouples.

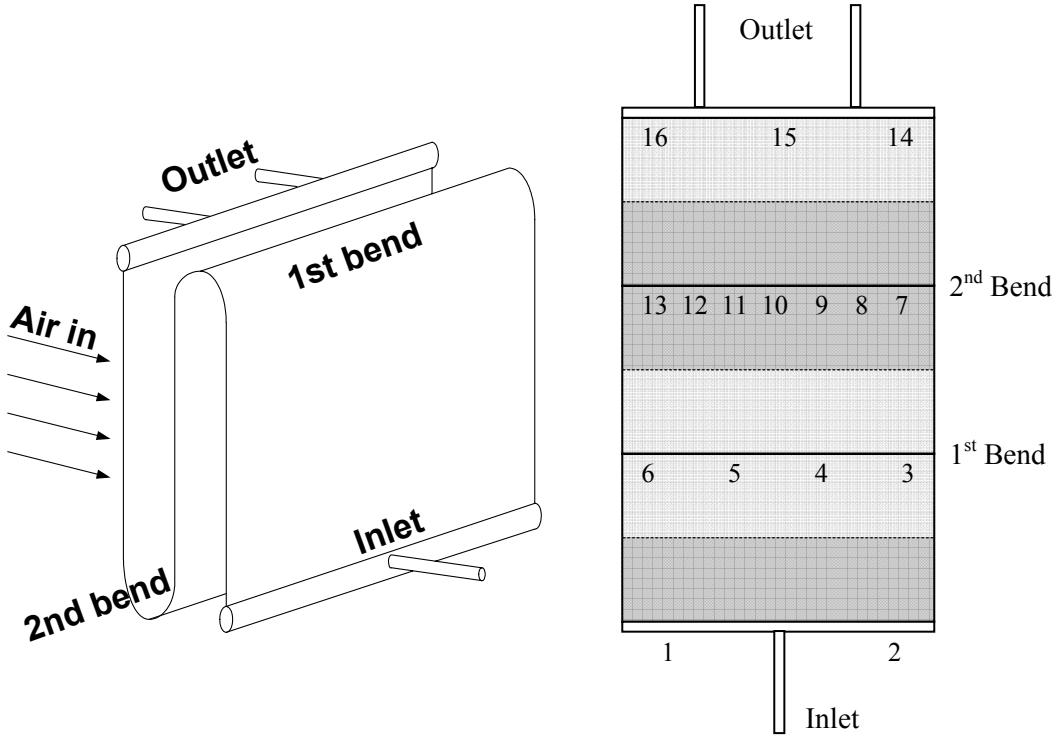

Figure B.3.1 Geometry of evaporator and the location of the numbered thermocouples

Uribe et al (20xx) determined the average metal temperature by calculating an area-weighted average and used to control Q. This was founded on the notion that each row of thermocouples on the bends and the headers accounted for a third and a sixth of the area respectively. In Figure B.3.1 the difference areas covered by rows of thermocouples are highlighted by the differently shaded areas. Theoretically this would give a very accurate average metal temperature of the evaporator. In practice, however a number of the thermocouples are not reliable, there are large differences with time (due to maldistribution and dryout) and the headers are too thermally massive accurately reveal rapid temperature changes. To avoid these problems of averaging metal temperatures in the evaporator, we looked at the both bends individually (i.e. all plots have both bend temperatures).

Appendix C: Experimental Data

The experimental setup was representative of a typical rapid cycling system so it could provide a knowledge base for rapid cycling design recommendations. Experiments were carried out to test different configurations to develop a further understanding of performance tradeoffs in rapid cycling. The experimental setup was similar to earlier work (Ilic et al. 2001), but included a microchannel heat exchanger and a high-effectiveness suction line heat exchanger instead of a conventional evaporator. To benchmark our rapid cycling tests, variable speed tests were performed to get a deeper understanding of system and component performance of the system under steady state conditions.

C.1 Single Cycle Analysis

Ilic et al. (2001) found that rapid cycling performance using a conventional evaporator yielded promising results. It showed that cycle periods as long as 10-20 seconds could produce COP's comparable to those achievable with variable speed compressors. Using conventional heat exchangers, dryout (superheating in the evaporator during the off-cycle) was a significant problem and degraded the performance for longer cycles. To reduce degradation of performance, a microchannel heat exchanger was used in conjunction with a suction line heat exchanger to increase the wetting of the evaporator walls.

Through actual experimentation with a best-available microchannel heat exchanger prototype (originally designed as a CO2 gas cooler) it was found that our microchannel evaporator was equally vulnerable to the evaporator dryout problem. While some of the losses observed in our tests such as evaporator pressure drop can be reduced with a better-designed microchannel evaporator, the data from this prototype nevertheless yielded valuable insights. Since the evaporator was still vulnerable to dryout, we were not able to lengthen the original cycle periods. Our focus therefore remained on shorter cycles (5-20 seconds) instead of the longer anticipated cycles (~20-80 seconds) explored by Ilic et al.

C.2 Transients

It was found that with a microchannel evaporator and the focus on shorter cycles the transients between the on and off cycles could not be neglected because they accounted for a significant fraction of the cycle period. Ilic et al. (2001) had defined loss terms in terms of separate on and off cycles which could not be applied to our data. For instance, their pressure drop loss term was defined as the pressure drop in the evaporator during the on cycle only, and was based on the assumption that there was no evaporation during the off cycle. Figure C.2.1 shows the pressure drop in the evaporator for a ~5 second and a ~20 second 40% runtime case. Unfortunately this prototype had been designed for CO_2, so its performance in our R22 system was suboptimal (e.g. the pressure drop was too large). Nevertheless the trends were similar and the lessons from this prototype can be generalized to appropriate designs.

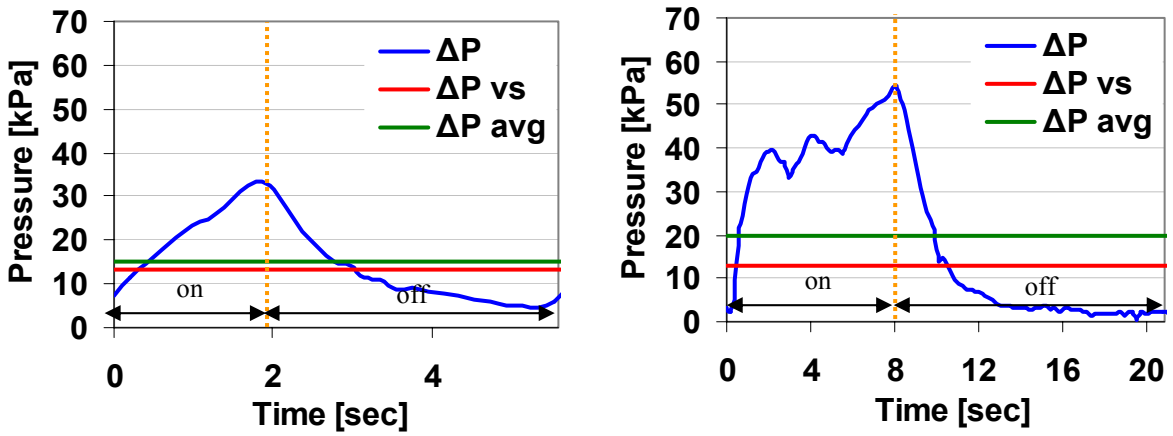

Figure C.2.1 Evaporator refrigerant pressure drop profiles of a 40%, ~5 second and ~20 second cycle

Figure C.2.1 showed that blending of the on- and off-cycle results in much lower average on-cycle pressure drop, which was closer to the variable speed pressure drop. With the conventional evaporator the pressure drop had occurred almost exclusively during the on cycle. The evaporator pressure drop measurement shown in Figure C.2.1 was a representative case in which this type of on/off cycle blending occurs. Other measurements showed that the changes in metal temperature, air temperature, and saturation pressure were reduced in shorter cycles. These results were expected as very short cycles started to resemble variable speed operation.

Comparing the two graphs it was immediately obvious that there was a transient involved, which caused the pressure drop to rise over the course of the first ~10 seconds and drop off in ~5 seconds after the compressor stopped. The reason for the off-cycle transient was most obvious; it took some time for the remaining liquid in the evaporator to boil after compressor shutdown, during which time it continued to reduce the temperature of the metal. The on cycle transient took longer to build up because the steady state liquid inventory needed to be re-established in the evaporator after the off-cycle depletion. This took up to 20 seconds (based observations in much longer cycles) especially when the off cycle was also much longer. In longer cycles there was dryout in the evaporator, warming its metal mass far above the saturation temperature, so flash boiling took place during the initial part of the re-wetting process as the metal was cooled towards the saturation temperature. In Figure C.2.1 this flash boiling was seen in the form of a superheat ‘bubble’ where the refrigerant temperature at the evaporator exit briefly deviated from the saturation temperature, because the dried-out metal had warmed during the off-cycle to exceed the saturation temperature and this region needed to move through the evaporator.

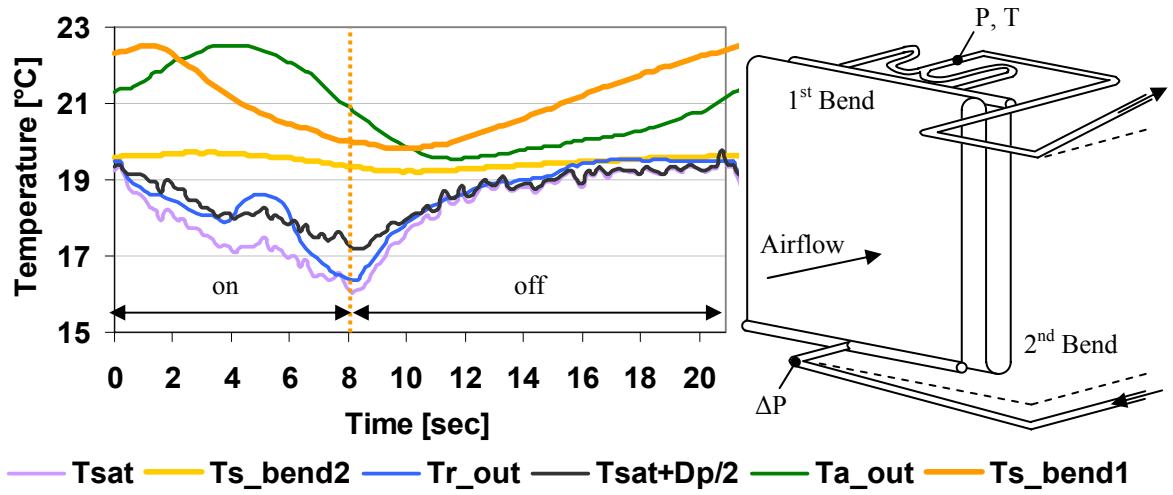

Figure C.2.2 Evaporator refrigerant, metal, and air temperatures for a 40 %, ~20 second cycle.

Note that in Figure C.2.2 the metal temperatures were measured at the tube return bends located between the three slabs that were isolated from the air stream. It was therefore likely that during the off cycle during superheated conditions, the metal temperatures in the face of the heat exchanger are hotter than those in the bends. During the off cycle temperatures in the first bend rose much quicker than those in the second bend, not only because the first slab meets the warmest air, but also because after the boiling slows down the refrigerant would drain from those tubes at the top of the heat exchanger.

C.3 Off cycle boiling

The superheat bubble only occurred in longer cycles if the off cycle heat transfer was high enough to raise the metal temperature above the saturation temperature. This was dependent on both the capacity which governed the airflow rate and the actual length of the off cycle. Through calculations of full speed steady state conditions it was found that about 20 g of liquid exist in the evaporator tubes at the start of the off cycle. There is probably liquid pooling in the outlet header below the tube ends which protrude nearly halfway up into the horizontal cylindrical header. If assumed half full of liquid, the outlet header contains an additional 15 g of refrigerant. The inlet header presumably contains more liquid as there could be pooling and stratification but the quality is also about 0.02 (~10% void fraction), meaning it would be 90% full of liquid, corresponding to approximately 27g, for a total of 62g. Figure C.2.2 shows the inlet tube carrying refrigerant upwards into the inlet header. Since the valve is ~0.2 m above the header inlet and the tube is ~95% full of liquid it is possible that additional liquid drained into the evaporator during the longest off cycles.

In Figure C.2.2, during the first four seconds of the off cycle (seconds 8-12) refrigerant mass boils off as is evidenced by the pressure drop transient in Figure C.2.1 since a positive pressure drop indicates flow out of the evaporator. The conservation of energy allowed estimation of the mass boiled in the evaporator tubes and headers. These calculations were based on the following equation for the off cycle

$$\int \dot{Q}_{air}\, dt = m_{boiled} h_{fg} + m_{metal} C_{metal} \Delta T_{metal} \qquad \text{(C.3.1)}$$

where the Q_{air} was determined by integrating the inlet/outlet air temperature difference over the length of the off cycle and the total metal mass was about 2.5 kg. Real time measurements of metal temperatures and air side capacity allowed the terms to be evaluated separately, and refrigerant mass to be calculated. It was clear that the refrigerant mass in the tubes of the evaporator quickly dried out since even the shortest off cycles boiled about 20g of refrigerant as shown in Table C.3.1.

In Figure C.2.2, the outlet air temperature rises due to the off cycle warming of the metal, decreasing the air side capacity accordingly. When dried out, the metal temperature in the middle of the face of the heat exchanger was probably ~2 degrees higher than the estimation suggested by the temperature in the first bend due to the fact that the bends are not in the airflow. Infrared images taken of the first slab showed the surface thermocouple rising 0.5 degrees/sec after dryout in the center face of the evaporator at high load conditions. Therefore the ΔQ_{metal} in Table C.3.1 is probably underestimated by factor of two but it is still a relatively small fraction of the total. The third column represents the remainder of the measured off cycle air cooling and is therefore overestimated by a relatively small percentage. Similarly in the fourth column the mass boiled in the evaporator to keep the air cool is probably overestimated by less than 10%. The estimates in Table C.3.1 are therefore generally consistent with the hypothesis regarding that dryout completely empties the tubes and part of the headers, thus leading to significant performance degradation.

Table C.3.1 Off cycle cooling

Cycle	Q_{air}	ΔQ_{Metal} (kJ)	$\Delta Q_{Boiling}$ (kJ)	mass boiled (g)
40% 2on-3.6off	1.4	0.0	4.9	26
40% 4on-6.9off	1.4	1.0	8.3	44
40% 6on-9.9off	1.4	1.5	11.9	63
40% 8on-12.9off	1.4	2.3	15.4	81
60% 3on-2.2off	2.1	0.2	4.3	23
60% 6on-4.3off	2.0	1.0	7.8	41
60% 9on-6.5off	2.1	1.7	11.9	63
60% 12on-8.5off	2.0	2.2	15.1	80
80% 4on-1.3off	2.7	0.0	3.5	19
80% 8on-2.3off	2.7	0.2	6.0	32
80% 12on-3.2off	2.7	0.8	7.8	41
80% 16on-4.2off	2.7	1.0	10.3	54

The increase in the metal temperature allowed us to theoretically deduce how much refrigerant mass would need to have been boiled. To make this calculation the delay in air side temperature difference was taken into account. While the metal temperature measurements were almost instant, the air outlet temperature was delayed by the travel time through approximately 1.5 m of wind tunnel before the temperature was measured as it passed through the nozzle. If the air velocities are assumed to be uniform throughout the wind tunnel there would be a 3.9 second delay at 40% capacity down to 1.9 seconds at 80% capacity. For very short (~5 sec) cycles there is almost no change in outlet air temperature and although the compressor cycles on and off, the metal and air temperatures are constant. The change in metal temperature was also a relatively rough estimate due to the fact that thermocouples were placed on a few individual tube bends which might not be ‘representative’ because they could be affected by

maldistribution. Therefore the amplitude of the metal oscillations indicated at the tube bends might be off by a factor of two. Table C.3.1 estimates the mass boiled during the off cycle of for the entire test matrix. The calculations showed that there is more liquid boiled than that calculated to be present in the evaporator and the headers in some of the cases. While this could just be because of the roughness of the calculations, one reason for this could be that there is some drainage from the pipes upstream and downstream into the evaporator.

The transient nature of the evaporator liquid inventory is an important concept to rapid cycling. Consider for example the hypothetical case with only one second of off cycle. Since evaporation at full speed is ~22 g/s, it is likely that the evaporator tubes would almost dry out during a 1 second off cycle. Since the metal temperature would have no time to rise very far above saturation before the start of the on cycle there is no chance for superheat regions to occur. The pressure drop in the evaporator closely approaches that of variable speed operation because of the boiling that continues during the off cycle, because the headers are thermally connected to the headers. The liquid inventory in the tubes would be quickly re-established during the next on cycle.

From the energy balance it was found that the evaporator boiled off at least ~20 g during even the short off cycles. However it was found that the overall pressure increase in the low side did not reflect this same amount of boiling. During the off cycle the low side of the system was a completely closed system because solenoid valves isolated the system between the expansion valve and the compressor. The pressure increase accounted for a maximum of 6 grams liquid boiled during the off cycle. This indicated that although air is cooled by the boiling in the evaporator during the off cycle, some of that saturated vapor immediately condenses elsewhere, either at the interface of the liquid in the inlet and outlet headers or more likely the 5 m long suction line heat exchanger. Since the suction line heat exchanger is very effective, at the end of the on cycle the liquid line outlet and two-phase inlet are at almost the same temperature. As the saturation temperature is raised during the off cycle as liquid boiled in the evaporator, condensation occurs on the cold end of the well insulated suction line heat exchanger which is now at saturation pressure. For a case with a very long (~100 second) off cycle it was found that the metal temperature in both bends keeps rising much higher than the saturation temperature. The saturation temperature cannot keep tracking the metal temperature in the evaporator because of the condensation in the SLHX (it rises slower than the metal temperatures). During the next on cycle, the condensation had a negligible effect on the inlet quality of the evaporator, presumable because the thermal mass of the liquid in the suction line heat exchanger was large enough to absorb the condensation penalty.

C.4 On Cycle Recovery

Metal temperatures also exhibited transients similar to the trends in pressure drop as the liquid inventory was re-established in the evaporator during the on cycle. It would be expected that the maximum temperature would occur at the end of the off cycle and the minimum at the end of the on cycle but there was a lag. Figure C.2.2 showed that in the ~20 second cycle the maximum temperature in the first bend occurred about 1.5 seconds into the on cycle, while the maximum did not occur in the second bend of the evaporator for about 3 seconds into the on cycle. The evaporator outlet air temperature lagged even further and it took almost 4 seconds to reach a maximum (in the 40 % case). These delays reflect the time required to replenish the evaporator's refrigerant inventory (at 20 g/s) and to cool the thermal mass of metal, some of which had been heated far above the saturation temperature

during the off cycle. In longer cycles with a long off cycle, such as figure C.2.2 the evaporator at the start of the on cycle is presumed to be dried out.

The delay in temperature drop in the first and second bend of the evaporator indicate the time it takes for the saturation 'front' to pass through. The front slab at steady state conditions contains about 13g of liquid refrigerant, based on void fraction calculations in a steady state model. When the on cycle starts liquid is pushed into the front slab at 20g/s. For the first second most of this went into cooling the metal through flash boiling. As soon as boiling starts to occur in the first bend, the temperature there starts to decrease (but is not yet at steady state), which takes 1.5 seconds for the front slab. Figure C.4.1 shows IR camera pictures taken of the front slab as this front moved through the first slab in ~1.5 to 2 seconds. In this 20 second 40% capacity cycle, there was still boiling from the inlet header keeping the bottom area cool though the off cycle.

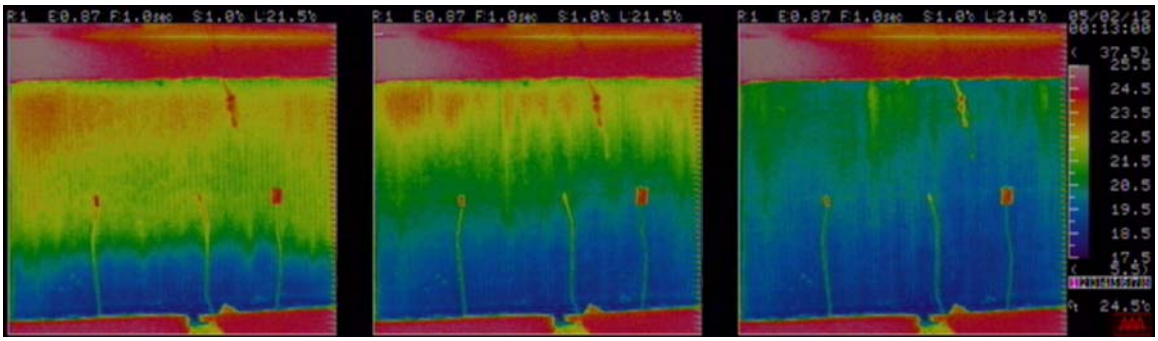

Figure C.4.1 Infrared picture sequence of the first three seconds of the front slab of the evaporator of a 20 second 40% cycle.

The second slab of the evaporator is not as hot and does not take as much liquid refrigerant to bring it down but since it is located after the first slab (where a lot of boiling occurs) it takes an additional 1.5 seconds for this temperature to start going down. IR pictures taken by Uribe et al. (2003) in a counter flow configuration showed that the upwind slab did not start cooling until 4 seconds into the on cycle, because quality was higher and refrigerant inventory lower.

C.5 Transients in different capacity fractions

Because the loss mechanisms involve non negligible transients in short cycles, we must use a different approach to quantify their effects. To identify and quantify the loss mechanisms observed in our experiments, ~200 second averages in performance comparisons were used.

When looking at different runtime fractions, in Figure C.5.1 compared to Figure C.2.1, the differences between variable speed operation and cycling operation were even smaller. In the ~ 5 second cycles, counter-intuitively, average pressure drop in the variable speed case was slightly larger than the rapid cycling case, and its temperature lift was slightly larger since the effective evaporator area was reduced due to maldistribution. This was where some of the overall performance benefits discussed later came from.

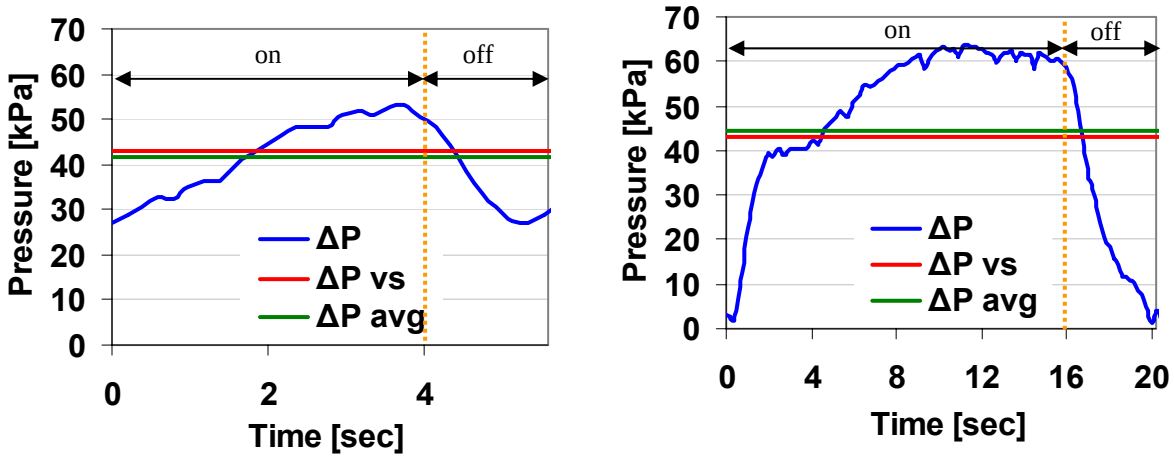

Figure C.5.1 Evaporator refrigerant pressure drop profiles of an 80%, ~5 and ~20 second cycle.

Table C.5.1 On and off cycle evaporator pressure drop

	on (sec)	off (sec)	ΔP_{on}(kPa)	ΔP_{off} (kPa)	%on	%off
40%	2.0	3.6	20	13	47%	53%
40%	4.0	6.9	27	10	62%	38%
40%	6.0	9.9	35	10	68%	32%
40%	8.0	12.9	38	9	71%	29%
60%	3.0	2.2	31	27	61%	39%
60%	6.0	4.3	35	18	74%	26%
60%	9.0	6.5	40	13	81%	19%
60%	12.0	8.5	43	11	85%	15%
80%	4.0	1.3	42	39	77%	23%
80%	8.0	2.3	46	34	82%	18%
80%	12.0	3.2	48	29	86%	14%
80%	16.0	4.2	51	22	90%	10%
VS 40%			12			
VS 60%			25			
VS 80%			43			
100%			59			

The evaporator pressure drop gives a very rough indication of the amount of refrigerant that is evaporating at any given time. For the shortest cycle periods the off cycle accounted for a larger percentage of the boiling. In the shortest 40 % cycle, there appears to have been more total boiling during the off cycle than the on cycle. In these very short cycles, during the on cycle the liquid inventory is re-established in the evaporator and the saturation temperature is brought down. As can be seen in the pressure drop profiles, the pressure drop at low-load conditions is less than high loads. Moreover it is generally only slightly higher than VS operation.

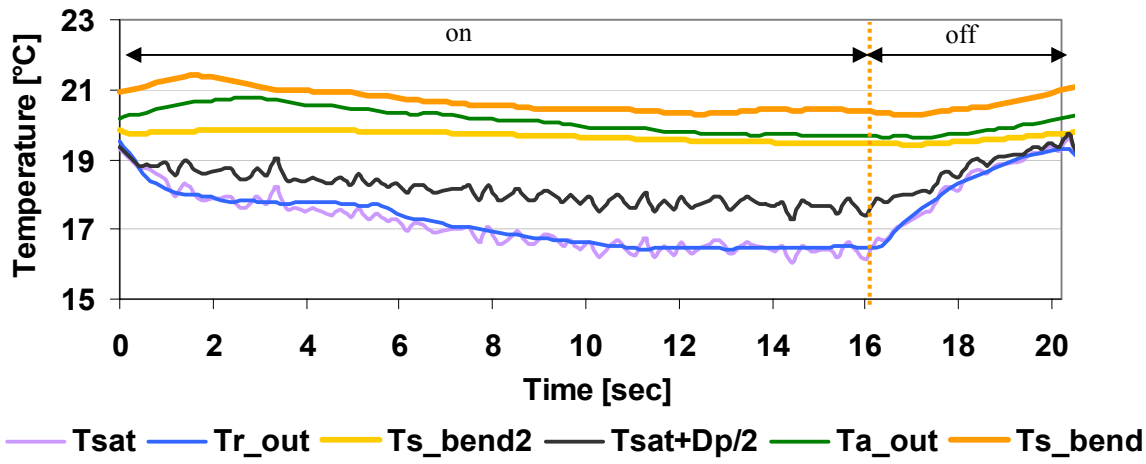

Figure C.5.2 Evaporator refrigerant, metal, and air temperatures for a 80 %, ~20 second cycle.

It is important to note that during even during these longer cycles, the actual duration of the off-period was relatively short since it had an 80% runtime. This reduced the dryout in the evaporator as evidenced by the absence of a superheat bubble. There could still have been some level of dryout in the evaporator, but it was small enough so that it did not produce a superheat 'bubble' at the exit. Due to the relatively short off cycle the amplitudes of oscillations in all the measurements were smaller. When moving to even shorter cycles this was especially evident as shown in Figure C.5.3 and Figure C.5.4 which compare the profiles of metal, refrigerant and air temperatures between a ~5 second cycle and variable speed operation.

While the superheat 'bubble' is obvious in cycles with a long off cycle, superheated regions may also form in the evaporator during shorter off cycles. However they may not be detected if the vapor is cooled again to a saturated state by passing through a wetted region of the evaporator tubes or outlet header and outlet tubing which are upstream of the immersion thermocouple. During long off cycles it is likely that at least all the refrigerant from the tubes and the headers is evaporated. During these long cycles it was found that the superheat bubble does not pass completely through the evaporator until approximately 6-7 s into the on cycle at any capacity fraction. Therefore when cycle periods were short, many of the on cycles were not long enough for the superheat bubble to pass through, this added to the blending of the on and off cycles. Additionally, after the initial off-cycle boiling depleted the ~13g of liquid in the front slab the first bend (located at the top) heats up much more rapidly then the second bend. While the second bend sees cooler air, it probably also holds liquid that drains down from the adjoining slabs. The appearance of the superheat bubble in the data is further repressed by 10-20 more grams of liquid in the evaporator outlet tubing upstream of the immersion thermocouple which could also evaporate after is has pooled during the off cycle, saturating any superheated vapor passing over it. There could also be more liquid entering the evaporator through the inlet header that was unaccounted for. It was also hard to see the superheat bubble when it started appearing since it was hard to detect when smaller than 0.5 degrees.

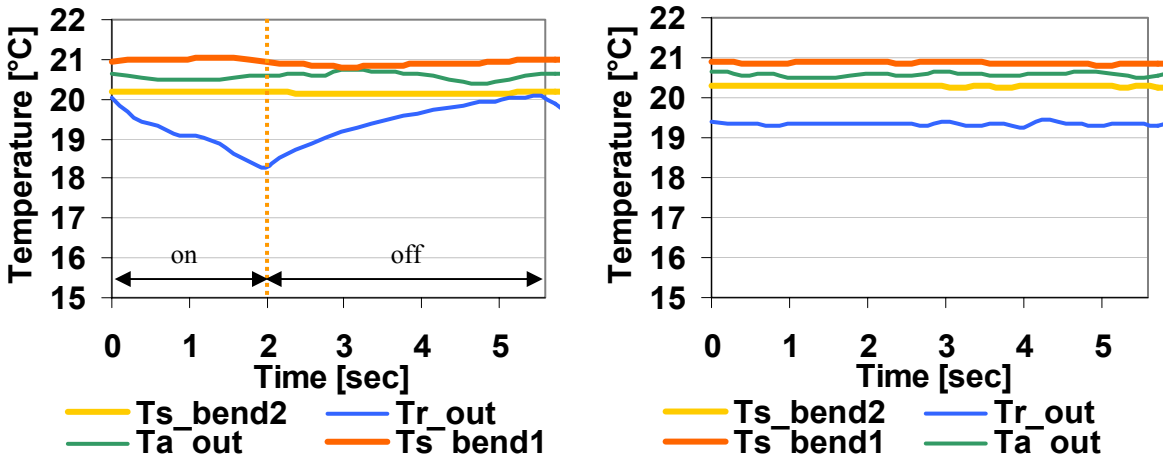

Figure C.5.3 Metal, refrigerant and air temperatures for 40% ~5 second and VS operation.

In Figure C.5.4, the refrigerant temperature remains well below the metal and air temperatures indicating that the evaporator probably remained completely saturated through the whole cycle. With the lower capacity fraction in Figure C.5.3 the refrigerant, metal and air temperatures were so close during the short cycle that perhaps some areas of the evaporator were superheated during the cycle. However there was not enough superheat to cause a detectable superheat bubble at the exit thermocouple.

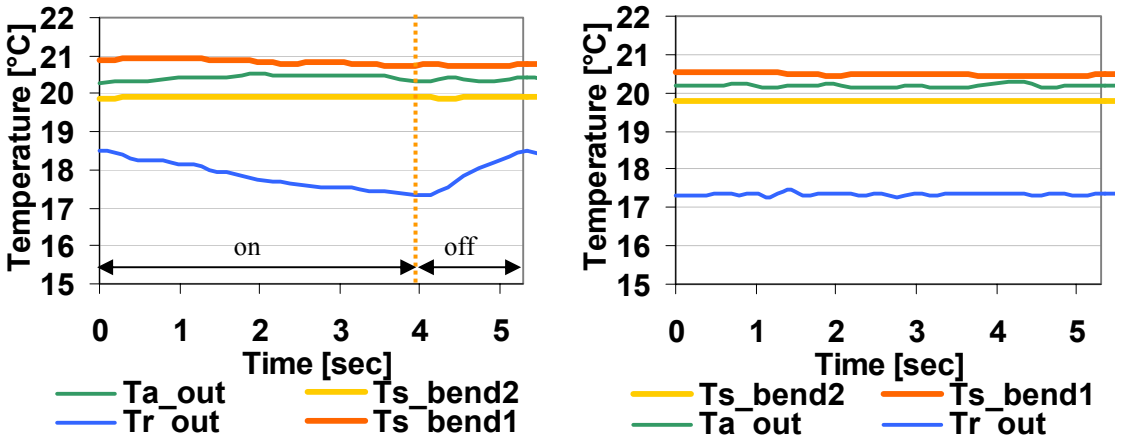

Figure C.5.4 Metal, refrigerant and air temperatures for 80% ~5 second and VS operation.

From the figures above, it was evident that as cycles get shorter, they start to look a lot more like variable speed cases. Since evaporator capacity and the whole-cycle average air inlet and outlet temperatures were kept constant and air flow rates were kept constant, the average metal temperatures were also the same.

Table C.5.2 Cycle average metal temperatures

	on (sec)	off (sec)	T_{s1}(°C)	T_{s2}(°C)	T_{avg}(°C)
40%	2.0	3.6	21.0	20.2	20.6
40%	4.0	6.9	21.0	20.1	20.5
40%	6.0	9.9	20.9	19.8	20.4
40%	8.0	12.9	21.0	19.5	20.2
60%	3.0	2.2	20.8	20.1	20.4
60%	6.0	4.3	20.9	19.7	20.3
60%	9.0	6.5	20.9	19.4	20.2
60%	12.0	8.5	21.0	19.3	20.2
80%	4.0	1.3	20.9	19.9	20.4
80%	8.0	2.3	20.7	19.7	20.2
80%	12.0	3.2	20.7	19.9	20.3
80%	16.0	4.2	20.7	19.7	20.2
40% VS			20.8	20.2	20.5
60% VS			20.5	19.8	20.1
80% VS			20.4	19.8	20.1
100% VS			20.0	19.8	19.9

In Table C.5.2 the average cycle metal temperatures show that they are the same as variable speed operation. The refrigerant temperature (and pressure) was the only transient which was not exactly like variable speed operation.

C.6 Comparison to conventional evaporator

When comparing the microchannel evaporator to the conventional copper tube and plate fin evaporator it was important to note several important differences. The system capacity was different; there was a tape heater after a small suction line heat exchanger in the conventional system while there was a large suction line heat exchanger (and no tape heater) in the microchannel system. The saturation temperature in the conventional system was held at about 10 degrees while that of the microchannel system was about 18 degrees because of the evaporator and compressor capacity differences. The following discussion compares the performance of the two evaporators during rapid cycling. The capacity fraction for the experiment with the conventional evaporator was 0.56 with a 10 sec cycle length while that of the microchannel was 0.58 with a 10.3 second cycle length.

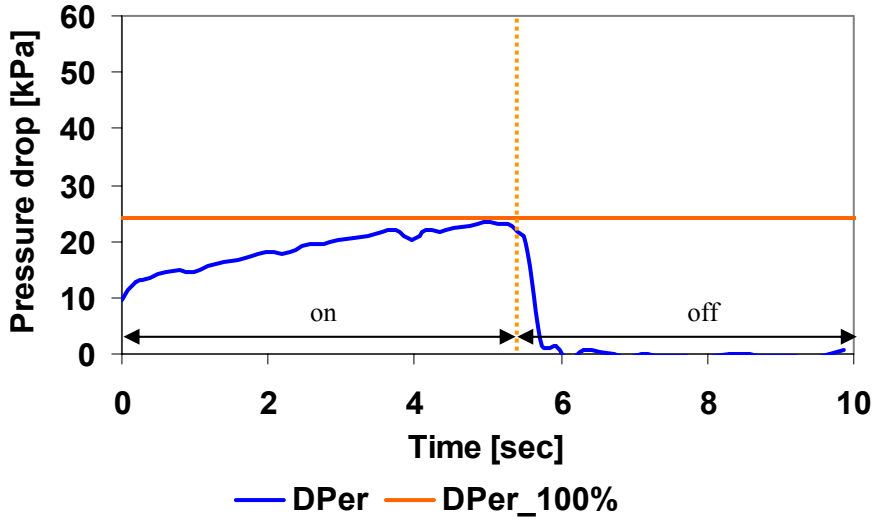

Figure C.6.1 Conventional evaporator pressure drop, 10 sec 0.56 capacity fraction.

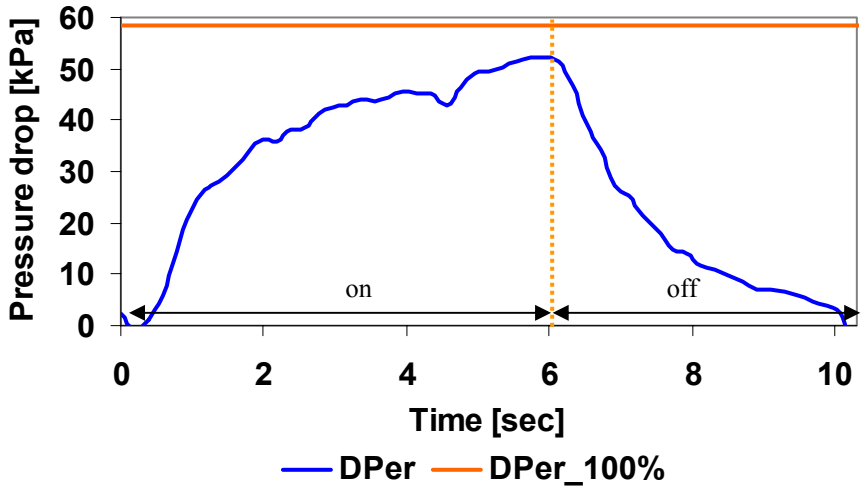

Figure C.6.2 Microchannel evaporator pressure drop, 10.3 sec 0.58 capacity fraction

One of the important differences was the amount of off-cycle boiling that occurred. The amount of liquid in the conventional evaporator at the start of the off cycle was calculated to be 230g using a simple finite element model based on the Zivi void fraction correlation. This is enough liquid to maintain full capacity of the system for 11 seconds in contrast to ~1 second in the microchannel evaporator. However Figure C.6.1 shows that the boiling in the conventional evaporator stops almost immediately, in about 0.4 seconds. The change of pressure in the low side indicated that approximately 15 g of liquid boiled during the off cycle, which correlated well with 0.4 seconds of boiling (steady state boiling ~40g/s). Figure C.6.3 shows that the reason for this was that the saturation temperature rose very quickly (within one second) to the metal temperature in the lower passes of the upwardly circuited evaporator (where most of the liquid mass would be). Since there was no more temperature difference between the

refrigerant and the metal, there was no more net boiling and from that point onward the cooling supplied by the system came from the slow warming of the metal and refrigerant in the evaporator. Since the conventional evaporator was much more thermally massive than the microchannel, it warmed slowly but the outlet air temperatures remained almost constant. The metal and the liquid in the evaporator heat up about 1.2 degrees Celsius during the off cycle, this effect accounts for about 3.4 seconds of the 4.4 second off cycle time at the constant capacity. During the other second of the whole 4.4 seconds off cycle some of the liquid vaporizes as the saturation temperature rises. While these are only relatively crude approximations, they encompass all the important mechanisms occurring in the evaporator.

It is important to realize there are probably other things that are affecting the evaporator performance. It is likely that the liquid refrigerant in the tubes seeped down to the bottom of the evaporator while some regions in the top of the evaporator the liquid film might evaporate off the tube walls and then superheat, and then condense in the bottom of the evaporator until it comes to equilibrium. This evaporation and condensation within the evaporator itself would not be detectable in the air side energy equation, nor would it produce a finite refrigerant pressure drop across the evaporator. Both, draining of refrigerant and 'heat pipe' effects were detected in the microchannel evaporator.

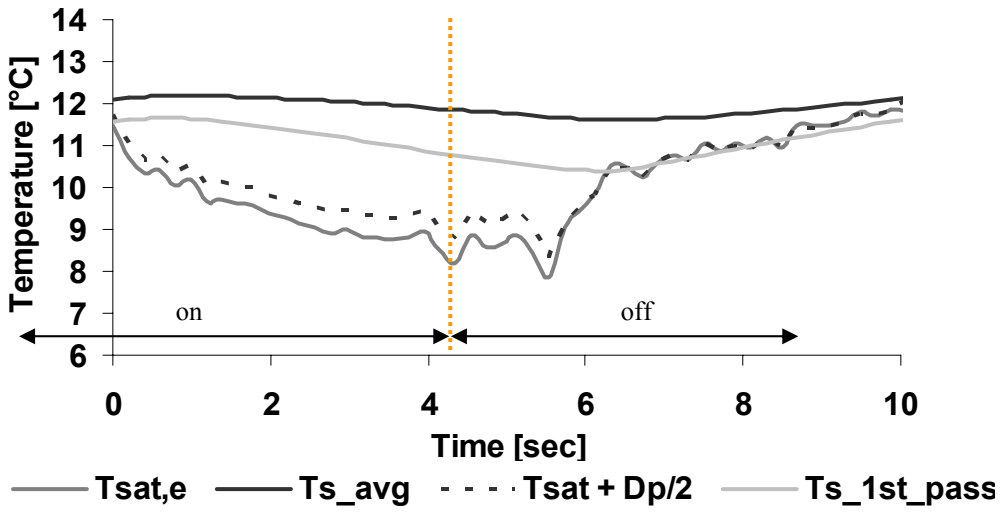

Figure C.6.3 Conventional evaporator temperatures, 10 sec 0.56 capacity fraction.

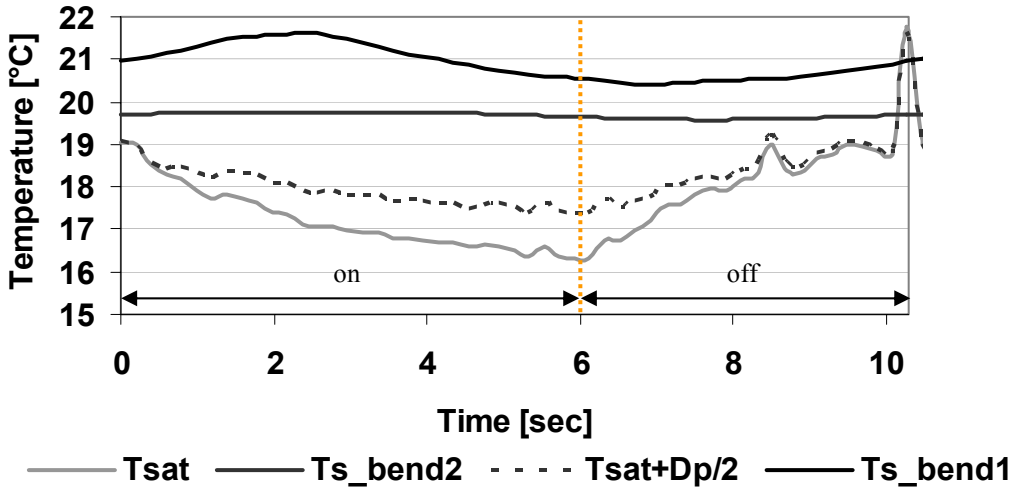

Figure C.6.4 Microchannel evaporator temperatures, 10.3 sec 0.58 capacity fraction (ignore noise spike)

Another relevant attribute of the two evaporators was the refrigerant side temperature difference during the on cycle. In the conventional evaporator the refrigerant temperature difference was almost isolated to the on cycle since the saturation pressure rose quickly after compressor shutdown due to a limited low side volume. Similarly, during the start of the on cycle the compressor quickly reduces the pressure in the low side and the refrigerant-side temperature difference is re-established. In the microchannel evaporator this was not the case as boiling slowly continued through much of the off cycle. It was originally thought that this evaporator would reduce the refrigerant side temperature difference by having a larger refrigerant side area as microchannel heat exchangers typically do. The refrigerant side area of this prototype evaporator was 0.53 m^2 in the tubes, and the conventional evaporator was 1.35 m^2. Since their cooling capacity differed by a factor of 2, therefore the refrigerant side temperature difference was approximately the same in both evaporators. However an optimally designed microchannel evaporator could have 3-4 times as much refrigerant side area.

C.7 Performance evaluation

Ilic et al. (2001) analyzed data from single "typical" cycles for analysis. While single cycles give detailed information about the dynamics of refrigerant, air and metal temperatures, longer (~200 second) averages, provide a better indication of overall system performance. In longer cycles it was also easier to filter the effects of transients during shorter cycles.

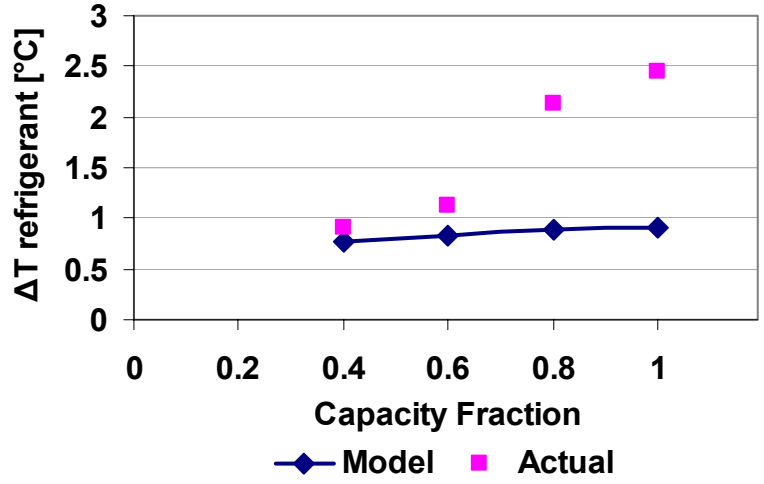

Figure C.7.1 Refrigerant side temperature difference

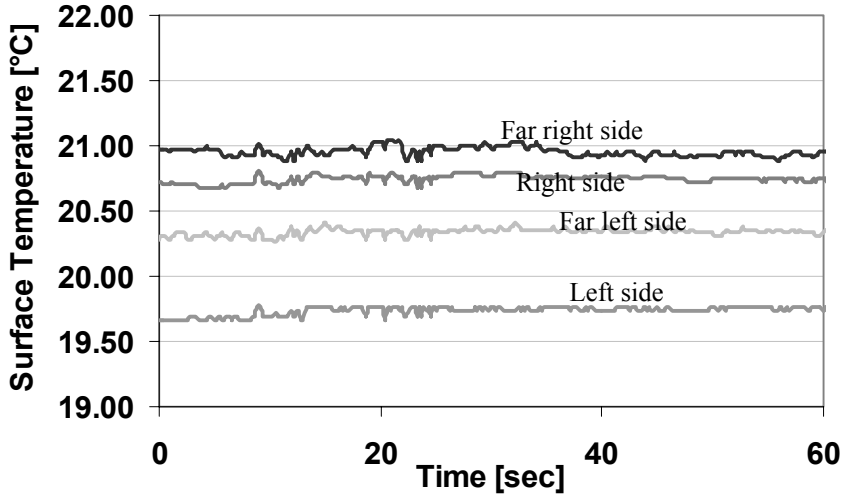

Figure C.7.2 Evidence of maldistribution from outlet air thermocouples.

It was found that during variable speed (steady state) operation there was significant maldistribution of refrigerant in the microchannel evaporator. This was evident in the refrigerant side temperature difference as capacity fraction increased from 0.4 to 1.0. The refrigerant side temperature difference was the difference between the average metal temperature (measured at the return bends between the slabs) and the refrigerant temperature in the middle of the evaporator. Figure C.7.1 compares the actual results with the results from a model using a heat transfer correlation for two phase flow in horizontal tubes and assuming uniform flow distribution.

The increased temperature difference suggests that there was maldistribution at the 0.8 and full speed capacity fraction. The air thermocouple grid downstream of the evaporator confirmed the occurrence of maldistribution as shown in Figure C.7.2. The primary reason was that the prototype evaporator's tube and header

diameters were sized for carbon dioxide, not a relatively low density refrigerant like R22. At higher refrigerant flow rates of 0.8 capacity fraction and full speed, (19and 22 g/s, respectively) the maldistribution was probably caused by the higher speed and pressure gradient of the refrigerant flow in the headers. This maldistribution did not occur in rapid cycling even though the mass flow rate was approximately that of full speed operation. During rapid cycling there was no similar evidence of maldistribution, perhaps because of bursts of refrigerant coming into the evaporator mixed the two phases more effectively, while steady state variable speed operation provided an opportunity for stratification in the inlet header.

C.8 Pressure Lift

The most important aspect of system performance was the amount of compressor work required for different capacities. Unfortunately there was no good way to compare measured compressor work during variable speed and rapid cycling conditions. Since our compressor was not designed for variable speed operation or for rapid cycling, the thermodynamic and motor efficiency of the compressor may differ between the two modes. Moreover, since the power spikes measured during rapid cycling were partially dissipative, it was not possible to separate out the work done and the work dissipated. Therefore our performance comparison was based on surrogate variables; the on cycle average pressure lift in the rapid cycling and variable speed systems. The comparison of pressure lifts also allowed us to focus on the system performance and other components rather than the internal workings of the compressor. The pressure lifts for capacity fractions from 0.4 to full speed operation were shown in Figure C.8.1.

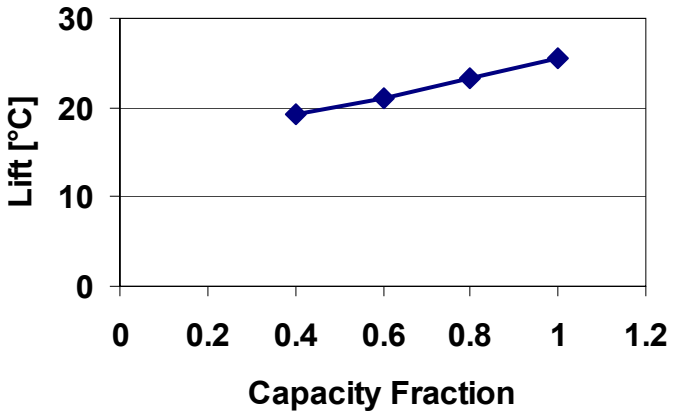

Figure C.8.1 Temperature lift at different variable speed capacity fractions.

The trend was almost linear but was slightly affected by the maldistribution at the 0.8 and 1.0 capacity fraction. In these cases the lift was slightly higher because maldistribution caused the effective area of the evaporator to be reduced, which created a need for a slightly lower saturation temperature to maintain capacity.

In cycling, as cycle lengths increase the average on-cycle evaporator saturation temperature decreases as shown in Figure C.8.2. As cycle length increases, the on cycle became longer and since the decline was not linear, this drove down the on-cycle average evaporator saturation temperature. The maximum saturation temperatures for each cycle increased slightly with cycle length due to the slightly increased off cycle lengths. The rate of saturation

temperature drop was independent of cycle length. Longer on cycles started to resemble completely steady state operation.

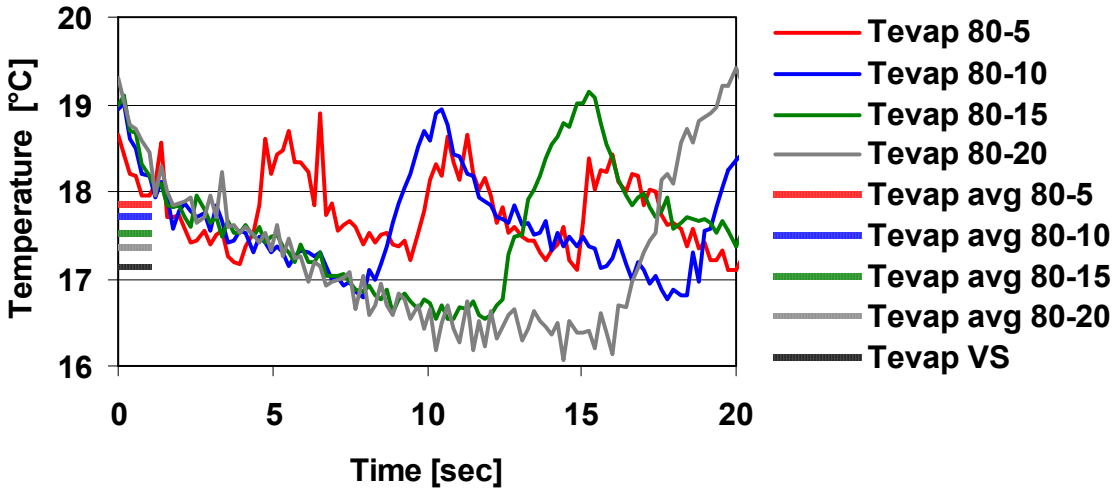

Figure C.8.2 Evaporator saturation temperatures for different cycle lengths at 0.8 capacity fraction.

To evaluate system performance under rapid cycling conditions the pressure lift was evaluated and contrasted with the variable speed cases. Two important trends were tracked: the effects on lift as cycle length and capacity fraction were varied independently.

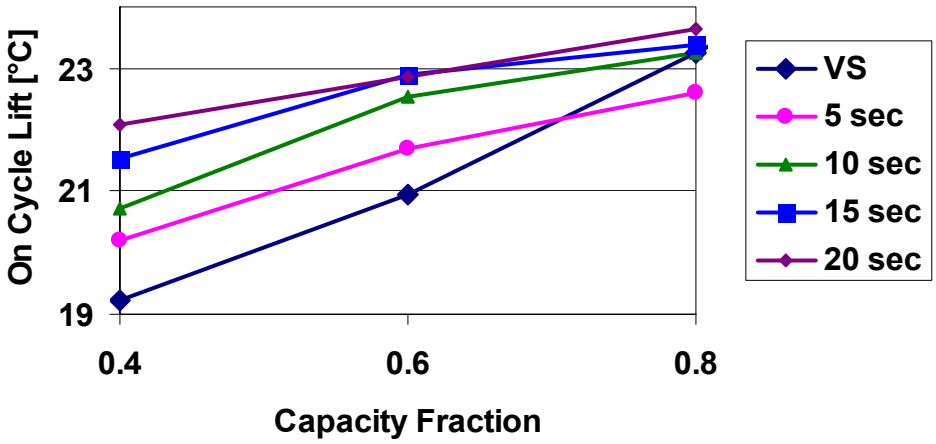

Figure C.8.3 Temperature lift at different capacity fractions.

The pressure lift increased with cycle length. Figure C.8.3 shows that lift also increases approximately 0.2 degrees for every additional 5 seconds of cycle length . It was also important to note that at 0.8 capacity fraction the variable speed case had a higher lift, probably due to the significant refrigerant maldistribution which was not observed in rapid cycling.

It is worth noting that the experimental facility was designed for 2-ton systems. Because there was no 2-ton microchannel evaporator prototype available, the results from experiments conducted with this 1-ton evaporator and compressor reflect the fact that the condenser was oversized by a factor of 2. Most of the benefit of rapid cycling and VS operation are attributable to the fact that the condenser is transferring heat ~100% of the time at a lower temperature difference. In these experiments the oversized condenser had already reduced condenser LMTD by a factor of 2, so there was less opportunity to save energy.

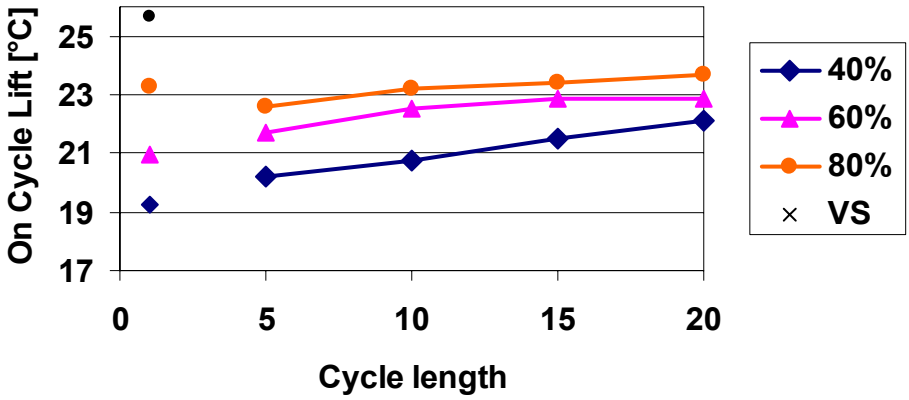

Figure C.8.4 On cycle temperature lift.

Figure C.8.4 was a plot of the average temperature lift during the on cycle of ~200 seconds of operation. When looking at the on cycle lift only, it was found that the temperature lifts are slightly higher than those of the whole cycle. In rapid cycling work is only done during the on cycle, and therefore the on cycle pressure lift is a more accurate reflection of the actual work done.

C.9 References

ACRC Research Highlights, Project 134, Designing and Optimizing Systems for compressor Rapid Cycling. Ilic S.M., Uribe T., Bullard, C.W. Hrnjak, P.S. February 2003.

Ilic, S. M.; Bullard, C.W.; Hrnjak, P. Effect of short cycling compressor modulation on refrigeration system performance. ACRC CR-43, 2001.

Incropera, F. P. and D. P. DeWitt, Fundamentals of Heat and Mass Transfer, John Wiley and Sons, New York, NY, 1996.

Kirkwood, A.C.; Bullard C.W. Modeling, design, and testing of a microchannel split-system air conditioner. ACRC TR-149, 1999.

Souza, A. and M. Pimenta, "Prediction of pressure drop during horizontal two-phase flow of pure and mixed refrigerants", In: J. Katz and Y. Matsumoto, editors. *Cavitation and Multiphase flow*, New York, NY: ASME, FED-Vol. 219, pp.161-171, 1995.

Stoecker W. F and Jones J. W. Refrigeration and air conditioning. Second edition. McGraw Hill, New York, 1982

Uribe, T.; Bullard, C.W.; Hrnjak, P. Designing and optimizing systems for compressor rapid cycling. ACRC TR-43, 2003.

Appendix D: Data

This appendix includes a complete set of data for a 20 second cycle at 40 % capacity, with 8 seconds on and 12 seconds off. These results are for the microchannel (~1 ton) evaporator.

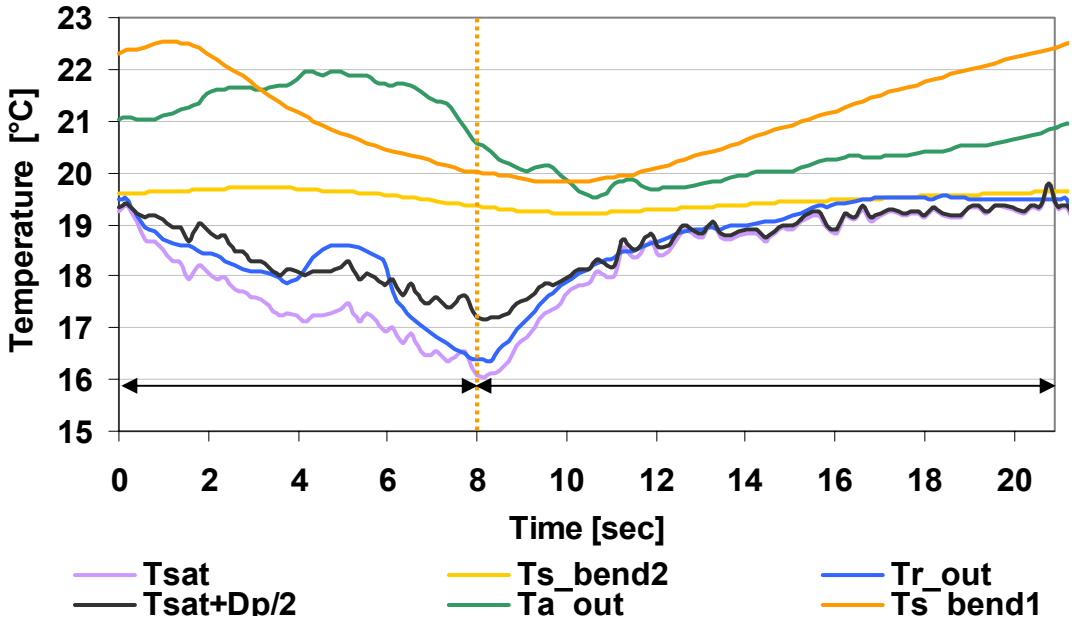

Figure D.1 Evaporator refrigerant, air and metal temperatures.

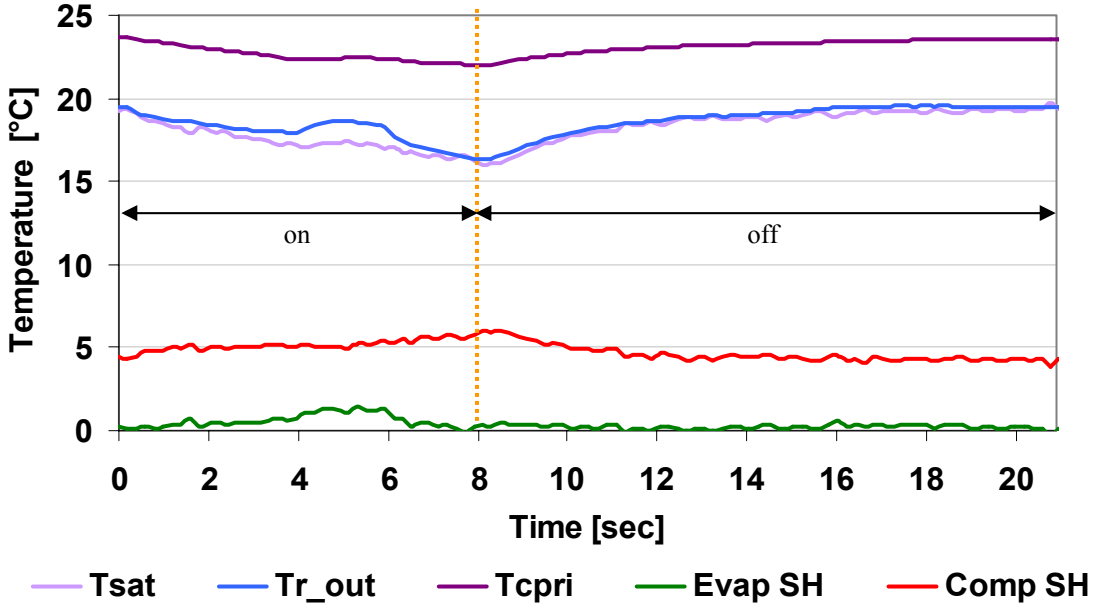

Figure D.2 Superheat at the evaporator exit and compressor inlet.

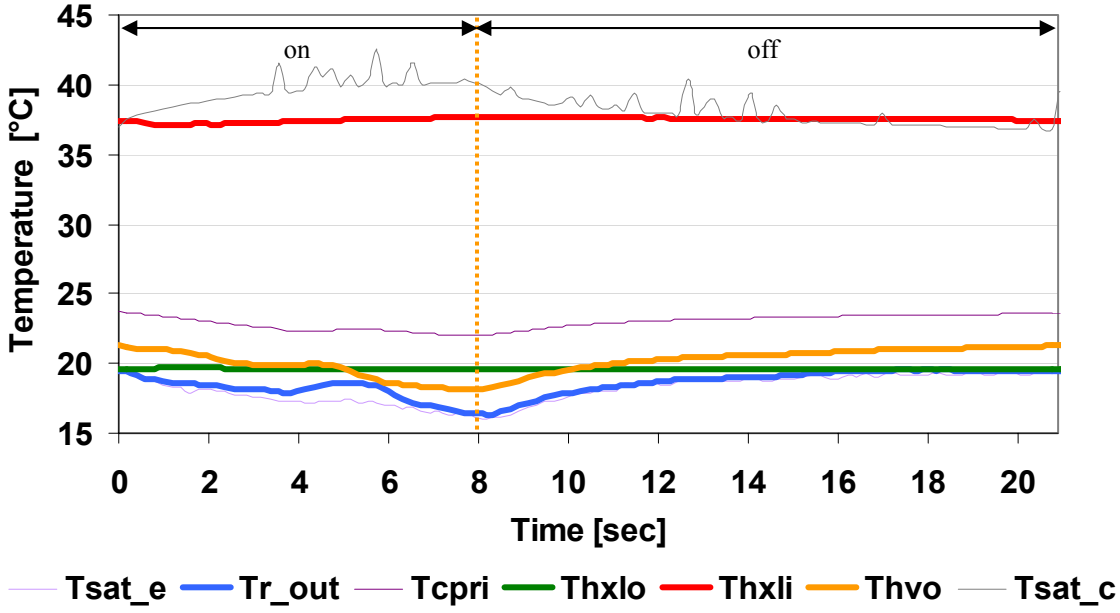

Figure D.3 Suction line heat exchanger (bold), and nearby (thin) temperatures.

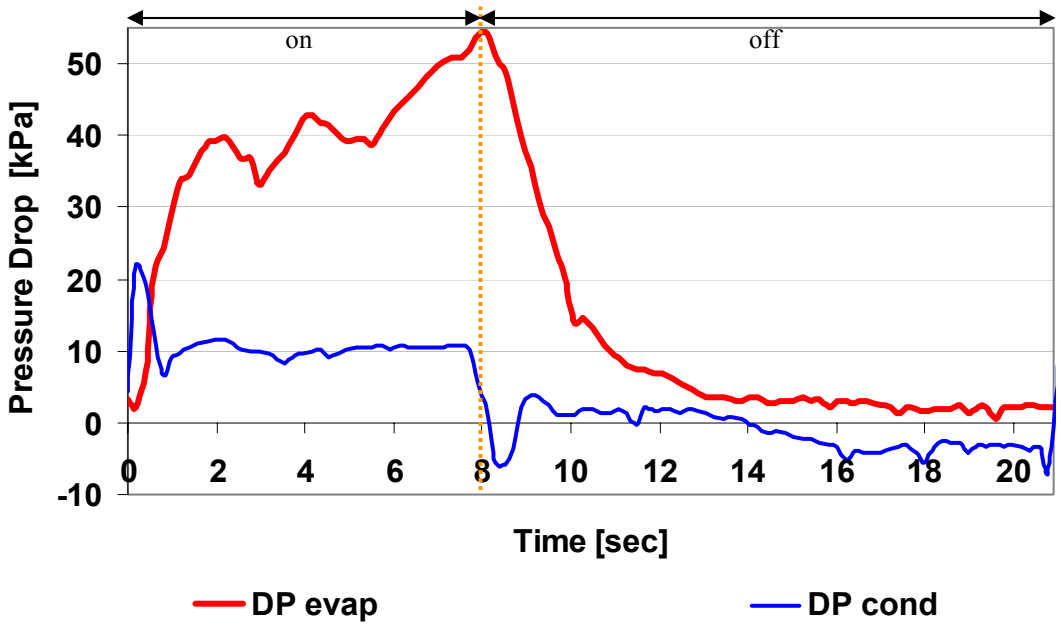

Figure D.4 Pressure drop in the evaporator and condenser

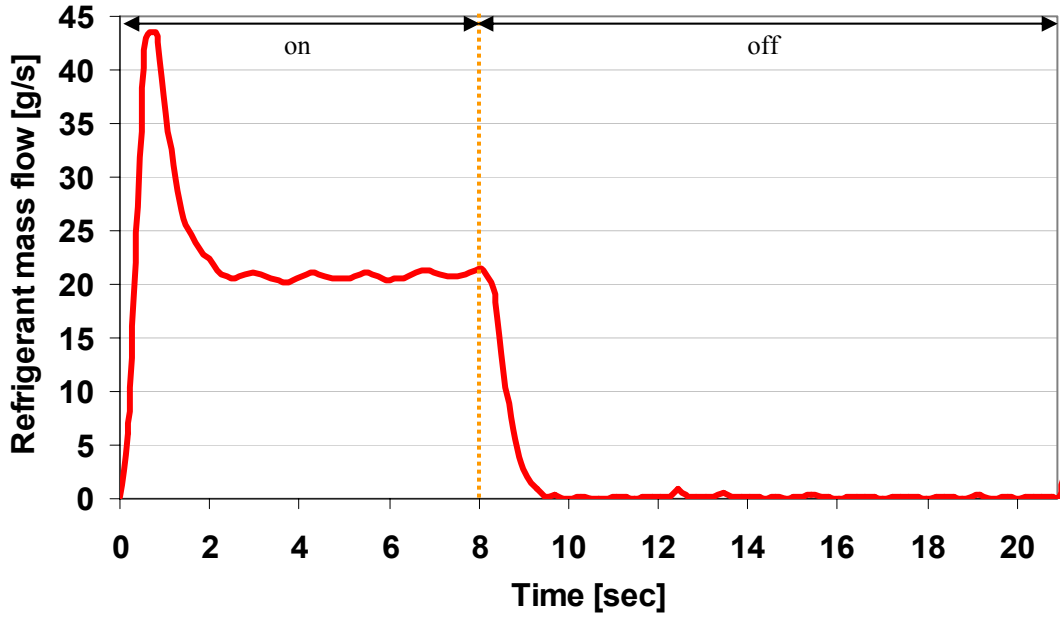

Figure D.5 Refrigerant mass flow rate (at expansion valve)

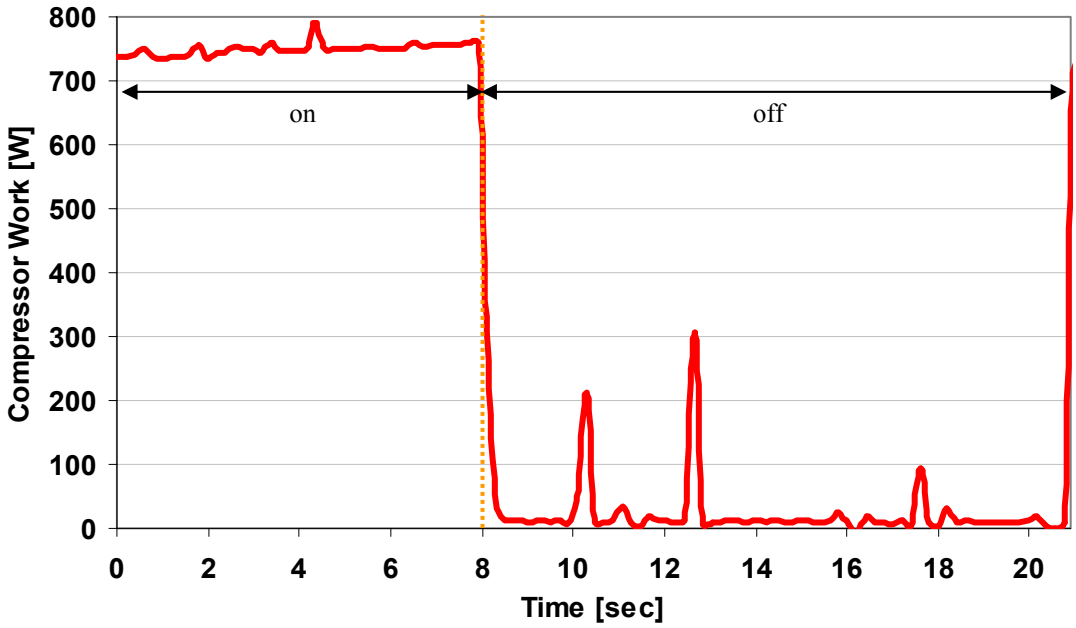

Figure D.6 Compressor power use.

Infra red pictures give a good indication of dryout and recovery of the liquid inventory in the front slab of the evaporator. The following is a series of images of a whole cycle, one picture taken every second.

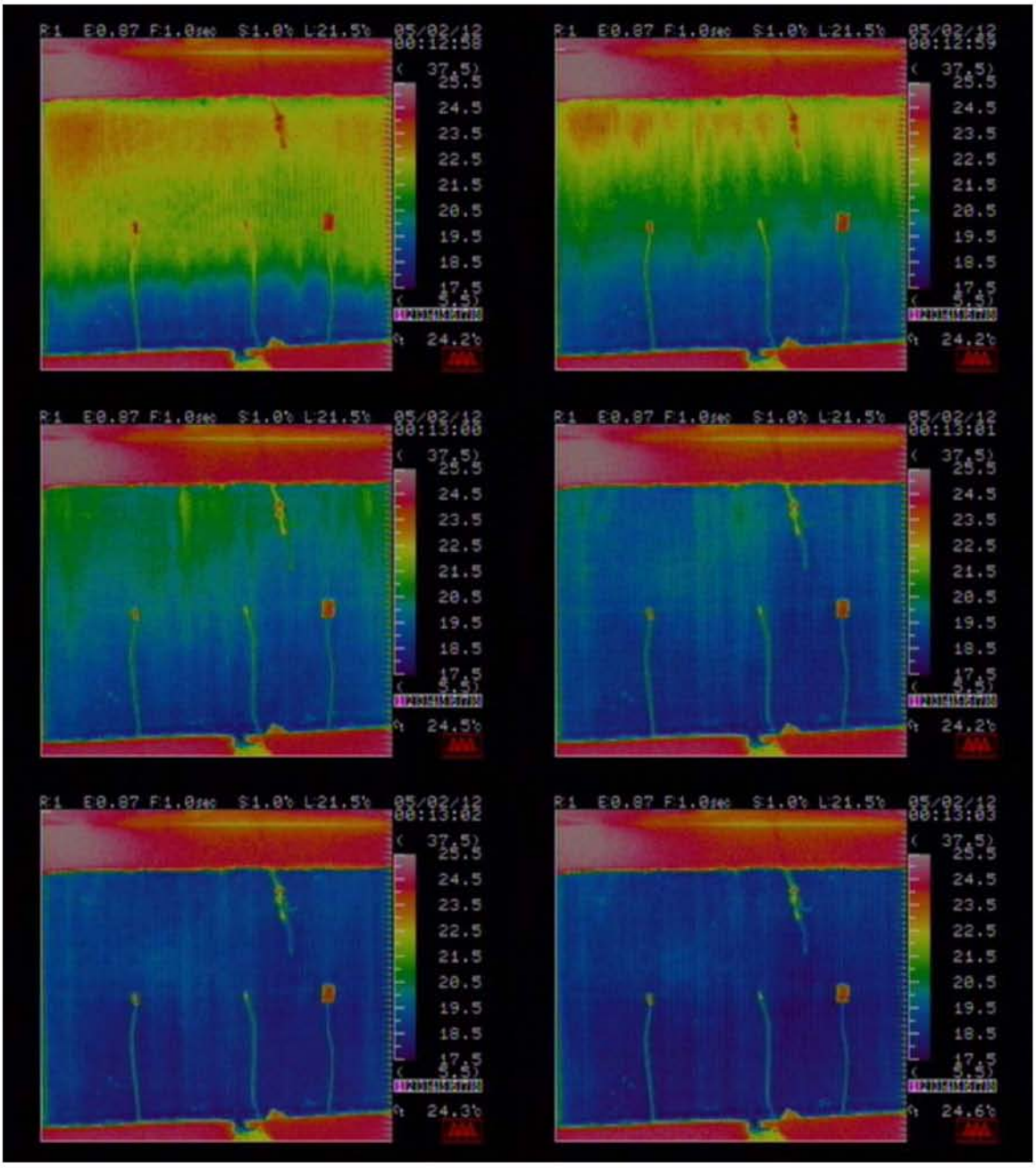
R1 E0.87 F1.0sec S1.0% L21.5% 05/02/12 00:12:58
R1 E0.87 F1.0sec S1.0% L21.5% 05/02/12 00:12:59
R1 E0.87 F1.0sec S1.0% L21.5% 05/02/12 00:13:00
R1 E0.87 F1.0sec S1.0% L21.5% 05/02/12 00:13:01
R1 E0.87 F1.0sec S1.0% L21.5% 05/02/12 00:13:02
R1 E0.87 F1.0sec S1.0% L21.5% 05/02/12 00:13:03
37.5
25.5
24.5
23.5
22.5
21.5
20.5
19.5
18.5
17.5
4.5
24.2%
24.5%
24.3%
24.6%

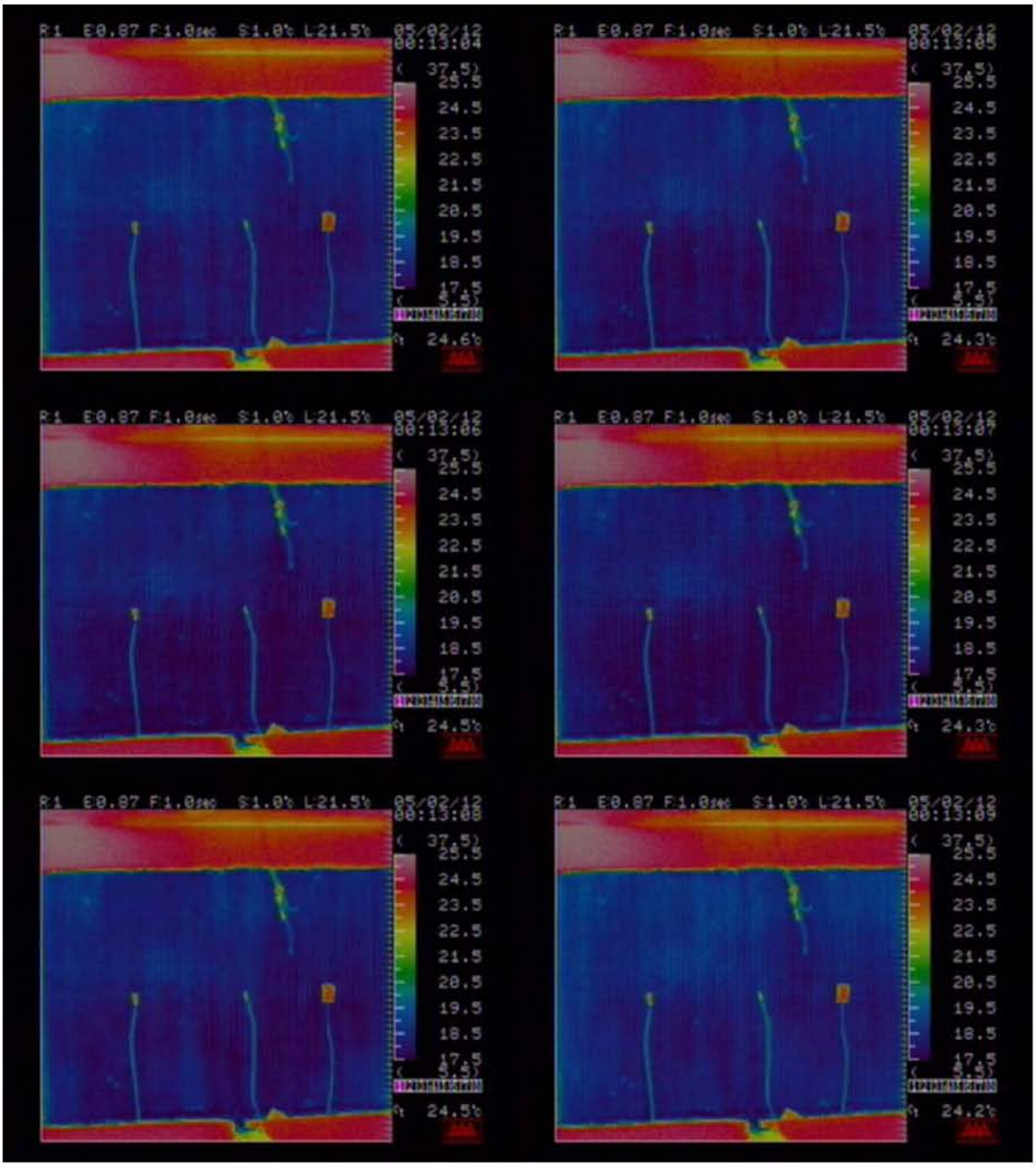
R1 E0.07 F1.0sec S1.0% L21.5% 05/02/12 00:13:04
R1 E0.07 F1.0sec S1.0% L21.5% 05/02/12 00:13:05
R1 E0.07 F1.0sec S1.0% L21.5% 05/02/12 00:13:06
R1 E0.07 F1.0sec S1.0% L21.5% 05/02/12 00:13:07
R1 E0.07 F1.0sec S1.0% L21.5% 05/02/12 00:13:08
R1 E0.07 F1.0sec S1.0% L21.5% 05/02/12 00:13:09
37.5
25.5
24.5
23.5
22.5
21.5
20.5
19.5
18.5
17.5
4.5
24.6%
24.3%
24.5%
24.3%
24.5%
24.2%

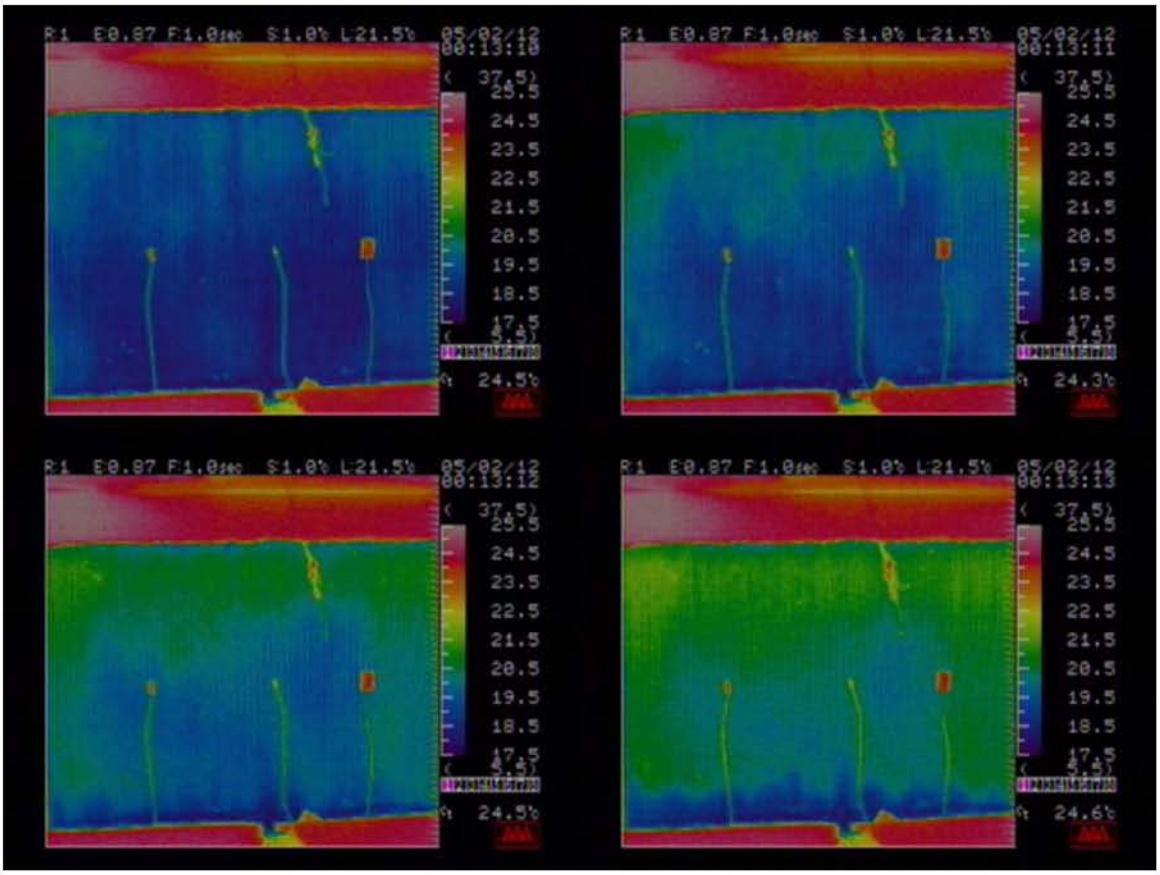
R1 E0.87 F1.0sec S1.0% L21.5% 05/02/12 00:13:10
37.5
25.5
24.5
23.5
22.5
21.5
20.5
19.5
18.5
17.5
24.5%
R1 E0.87 F1.0sec S1.0% L21.5% 05/02/12 00:13:11
37.5
25.5
24.5
23.5
22.5
21.5
20.5
19.5
18.5
17.5
24.3%
R1 E0.87 F1.0sec S1.0% L21.5% 05/02/12 00:13:12
37.5
25.5
24.5
23.5
22.5
21.5
20.5
19.5
18.5
17.5
24.5%
R1 E0.87 F1.0sec S1.0% L21.5% 05/02/12 00:13:13
37.5
25.5
24.5
23.5
22.5
21.5
20.5
19.5
18.5
17.5
24.6%

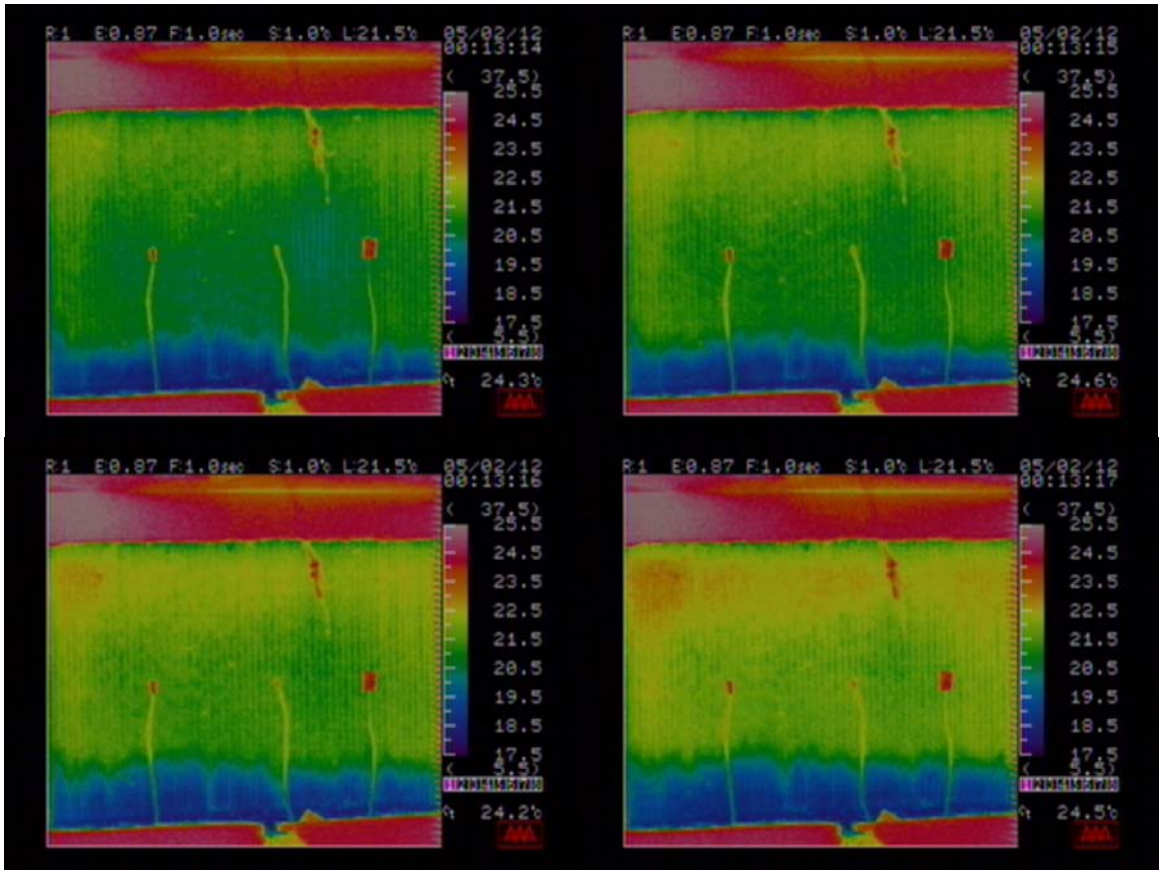

Figure D.7 Sequence of IR camera pictures taken every second for the 20 second cycle.

Appendix E: Condenser behavior during rapid cycling

In our evaluation of rapid cycling systems, the focus was primarily on the evaporator, to observe direct impacts on cooling capacity. The evaporator has to dehumidify, and can dry out with long off cycles while the condenser does not have these problems. Under rapid cycling conditions the condenser displays many of the same behaviors as the evaporator (but opposite). However, since the same condenser is in our experimental facility, for both the 2-ton (conventional evaporator) and 1-ton (microchannel evaporator) systems, the temperature differences are much smaller in the 1-ton system. Some valuable insights into condenser design can still be gained from the data on the 1-ton system. Firstly, to understand the some of the effects seen in the data it is important to understand the geometry as shown in Figure E.1. The most important thing to note is the location of the pressure and temperature measurements. The height of the liquid level between the pressure measurements and the receiver is also important.

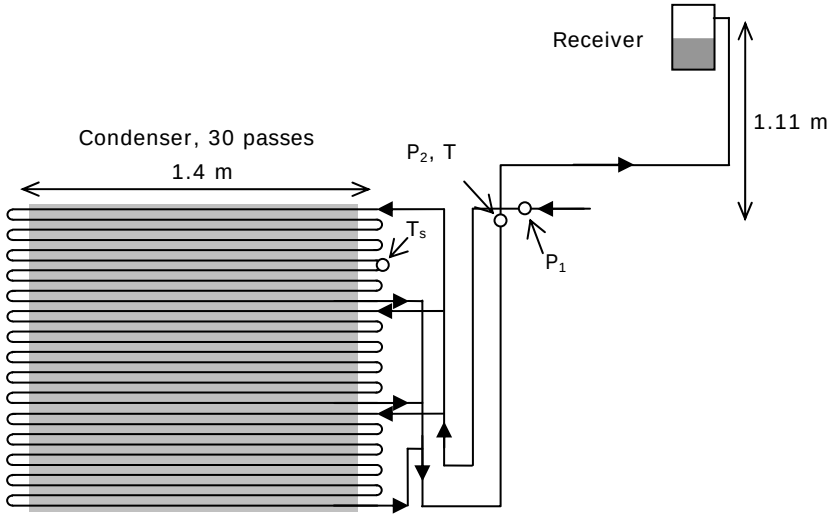

Figure E.1 Diagram of Condenser.

When analyzing the behavior of the condenser under rapid cycling conditions, the best place to start is with the condenser pressure drop, to help understand the refrigerant flow in and out of the condenser. Figure E.2 shows the pressure drop in the 2-ton system. The initial spike in the pressure drop was due to the additional condensed refrigerant, which condensed during the off cycle, having to be pushed out of the condenser, upwards to the receiver. The pressure drop quickly thereafter reaches steady state conditions very similar to that of full speed operation. At compressor shutdown, the pressure drop quickly falls to slightly negative values, causing the liquid column to flow back into the condenser. After this liquid column of liquid has drained into the condenser, there is no more mass flow leaving the condenser indicated by zero pressure drop. Figure E.3 shows the pressure drop in the 1 ton system which exhibits the same characteristics, except that its on-cycle magnitude is proportionally less due to the reduced mass flow.

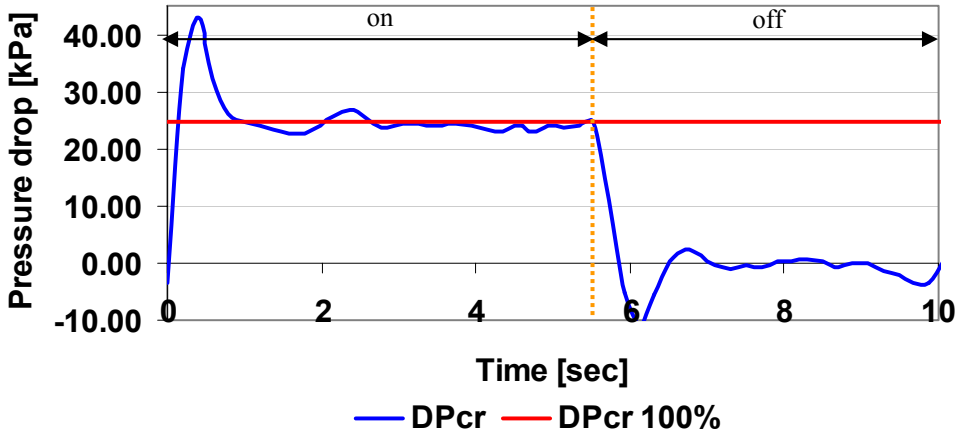

Figure E.2 Condenser pressure drop in ~2 ton system.

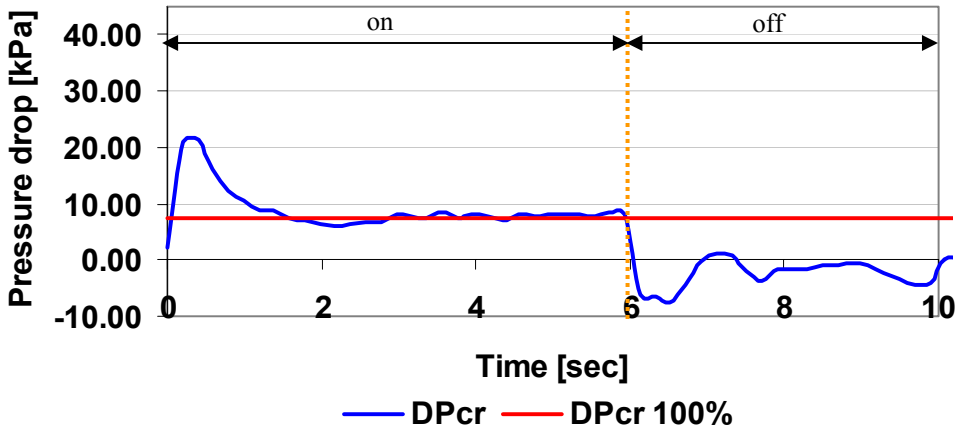

Figure E.3 Condenser pressure drop in ~1 ton system.

When analyzing the temperatures in the condenser during rapid cycling the biggest differences between the two systems is the fact that they are of different capacities (56% of 2 ton vs. 60% of 1 ton) with the same condenser and condenser air flow rate. While the behavior is expected to be the same in the 2 ton (Figure E.4) and 1 ton (Figure E.5) systems, the magnitude of the differences was expected to be slightly larger than half the magnitude of the 2 ton system in the 1 ton system. While the amount of refrigerant condensed during the on cycle differs by a factor of 2, the LMTD needs to be increased slightly in the 1-ton system to overcome the heat transfer resistance associated with halving the mass flow rate. During the off cycle, condensation continues although there is no more vapor entering the condenser. In the case of the 2-ton system this condensation takes about a second to reduce the refrigerant-side temperature difference until it is negligible. During the rest of the off cycle, the total thermal mass of the refrigerant and the metal governs the rate at which temperatures approach that of the ambient air. In the 1-ton system, the temperature differences are much smaller and therefore the refrigerant-side temperature difference is

also reduced quickly. Subsequent cooling during the off-cycle proceeds more slowly because the air-to-surface temperature is initially smaller, producing less driving force.

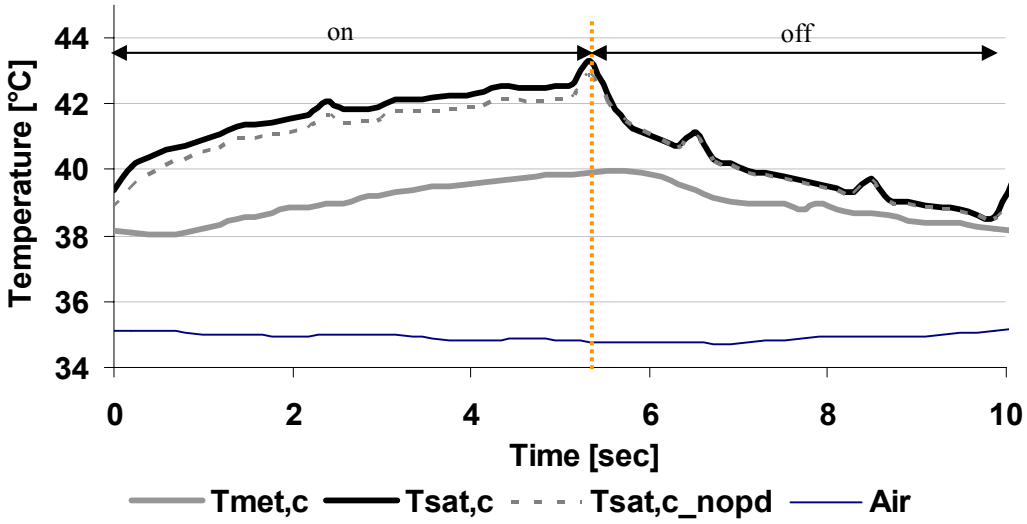

Figure E.4 Condenser temperatures in 2 ton system (conventional 2 ton evaporator).

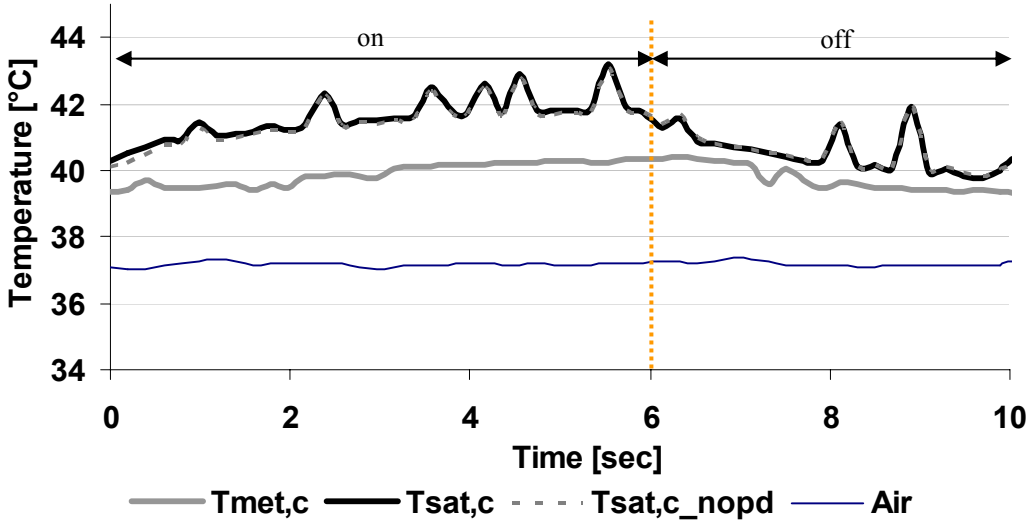

Figure E.5 Condenser temperatures on ~1 ton system (microchannel ~1 ton system).

Dryout and dehumidification requirements limit the duration of off cycles, while cooling done in the condenser during the off cycle is beneficial because it will just improve the quality of the refrigerant during the next on cycle. The analogy to evaporator dryout is the potential thickening of the liquid film on the condenser tube walls during long off cycles.. In this condenser designed for a conventional 2-ton system, the off-cycle change in internal of the refrigerant ΔU is ~9 kJ while the $mc\Delta T$ is ~21 kJ, hardly enough to sustain a 2-second off cycle at the design capacity, before approaching the outdoor ambient temperature. It seems clear that it would probably be impractical to add metal mass to the condenser due to its cost.

Appendix F: Water loops as thermal mass

This Appendix explores a potentially more cost-effective way to add thermal capacitance to a system, to achieve the benefits of a variable-speed (VS) system while avoiding the cost and inefficiencies associated with an inverter drive. The approach is to first estimate the potential energy savings, and then compare costs. Results indicate that the energy benefits, if any, are likely to be small, so an economic comparison was not performed.

Ilic et al. (2001) quantified the role of heat exchanger thermal capacitance in rapid cycling systems. The greater the thermal capacitance, the smaller and more symmetric are the surface temperature oscillations. Heat exchanger thermal capacitance can also lengthen cycle periods, thus increasing compressor reliability and diminishing the effect of dissipative power spikes. The results reported here have demonstrated that cycle length is always limited on the low side by the amount of wetted surface area in the evaporator. Even if a strategy could be developed for keeping the evaporator tubes wet during longer off-cycles so metal and refrigerant saturation temperatures could rise together, adding sufficient metal mass to the evaporator and condenser could be costly. The following analysis therefore explores the possibility of adding large amounts of thermal capacitance using a less costly material – a secondary water loop.

Secondary water loops would be required indoors and outdoors; Figure F.1 shows the outdoor loop where the goal is to increase efficiency by reducing condensing temperature, as in the case of VS systems. Since the indoor loop must meet latent loads there is no similar opportunity to reduce system temperature lift due to dehumidification requirements. In this system, a pump continually circulates water through a shell and tube condenser with a large water inventory and an air coil while the refrigerant loop operates in cycling mode. The advantage of this system is that the water in the loop provides the cheap thermal mass needed to achieve small symmetrical oscillations of the metal temperature in the condenser. The disadvantage, in addition to the cost of pumping power and the additional components, is a ~1 degree (at full speed) temperature lift penalty due to the approach temperature difference at each of the two additional heat exchangers on the high and low sides. Barnes and Bullard (2000) showed that water pumping power could be held to ~5% of compressor power in a comparison between a compact chiller system and a conventional split air conditioning system. Since refrigerant pressure drops and heat transfer resistance are already quite small in these compact brazed plate heat exchangers, the part-load temperature lift penalties associated with cycling (roughly a factor of $1/\mu$ larger than VS operation) are also quite small.

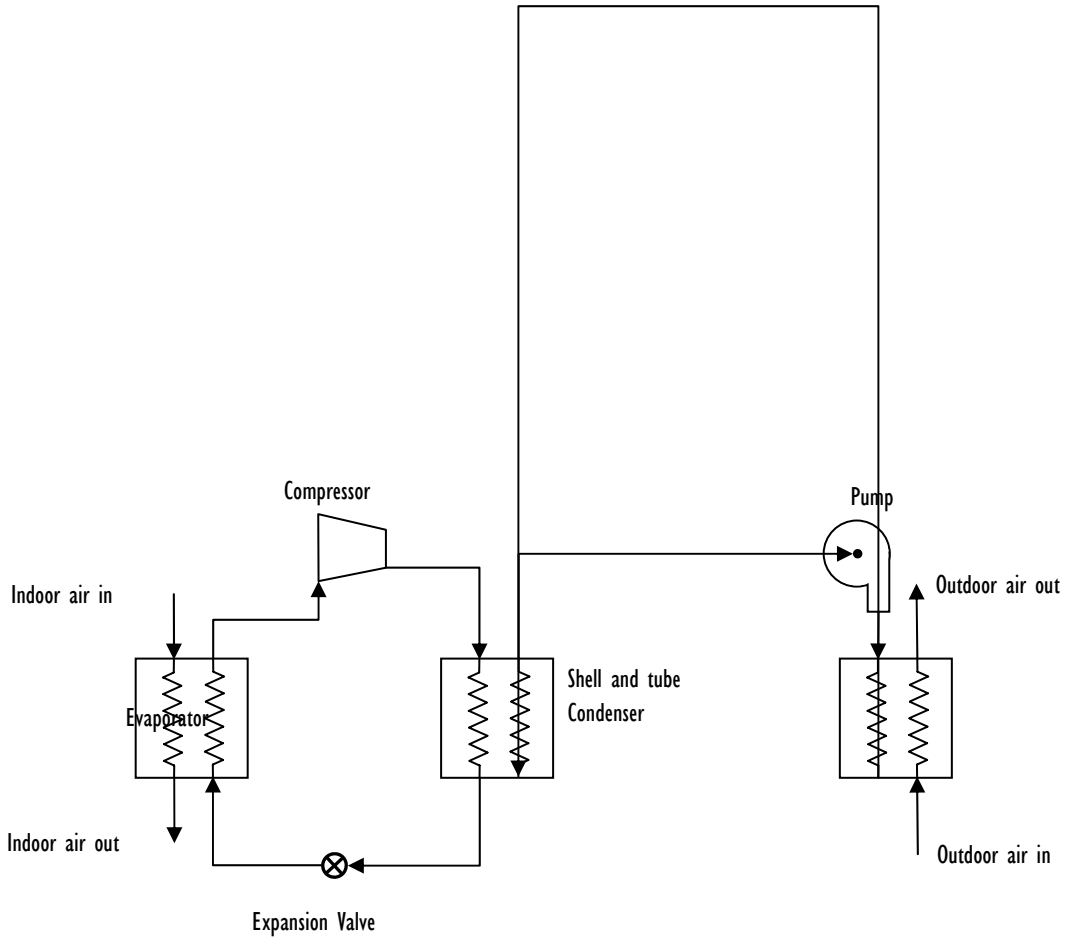

Figure F.1 Diagram of a secondary water loop with shell and tube condenser

The net energy efficiency benefit of this approach for increasing thermal capacitance of the system is therefore equal to the VS system's inverter losses, minus the additional power required to operate the secondary loops (pumps and additional compressor pressure lift). The amount of mass required is not large; a shell and tube condenser with a 50 liter water inventory would significantly increase the cycle length of a 2 ton system. If the amplitude of oscillations during a 20 second, 0.3 runtime fraction cycle would be 2 °C, adding the thermal mass of the 7 liters of water per kW in the evaporator the cycle could be stretched out to 300 seconds. These oscillations would be small, rising 1°C above and falling 1°C below the comparable variable speed temperature. At the maximum load (design) condition the system with the secondary loop will be less efficient than either a conventional single- or variable-speed system. The potential energy savings occur at low load where the LMTD across the outdoor air coil is reduced by a factor equal to the runtime fraction μ.

It is also clear that the secondary loop system will have a higher initial cost than a conventional system, but possibly lower than the cost of an inverter drive. The following analysis is therefore intended quantify the efficiency differences – the energy savings at part-load conditions – to determine whether they are large enough to warrant a detailed economic comparison.

These initial assumptions are conservative, in order to establish an upper limit on the efficiency penalty, so it can be compared to that of a variable-speed system. Recall that the motivation for considering rapid-cycling is to avoid the cost and inefficiency of an inverter drive and the refrigerant-side side heat transfer and pressure drop penalties at off-design conditions in a VS system.

The analysis focuses on relatively efficient systems, because that is the primary reason for employing VS or RC technology. Accordingly the irreducible temperature lift penalty at the evaporator and condenser is assumed to be only 1°C, which is actually not a difficult target for plate heat exchangers (Barnes and Bullard, 200x). Similarly it is assumed that the air-to-water approach temperature difference at the air coils is the same as that achieved in the two-phase zones of a VS system's air-to-refrigerant evaporator and condenser at the design condition – both are 1°C. While this is clearly an optimistic assumption, it is consistent with actual performance of very efficient systems. VS system efficiency is usually optimized for moderate outdoor conditions, and a pressure drop penalty is incurred at 35°C ambient by increasing compressor speed and refrigerant mass flux, thus minimizing the refrigerant-side temperature difference. The RC system, on the other hand, is optimized for a nearly-constant mass flux which also minimizes refrigerant-side resistance at the ARI-A condition.

The shell and tube heat exchanger system depicted in Figure F.1 is difficult to analyze because the water temperature would fluctuate. Moreover it may be optimal to use a much larger amount of water storage in order to extend cycle lengths to 10 minutes or more. Therefore initial calculations are performed for the physically more complex but analytically simpler system shown in Figure F.2 which shows the high side of a compact chiller system with brazed plate condenser connected to a secondary loop that circulates water to an outdoor air coil. The loop contains two storage vessels that allow water to be circulated continuously from one tank to the other, utilizing the air coil 100% of the time while the compressor (and brazed plate heat exchanger) operates in cycling mode. In this setup no water flows through the condenser during the off cycle, and the return water temperature is always constant. Cycle length is limited by the size of the water tanks, in this case with a water flow rate of 66 g/s, a 0.3 runtime fraction and a 300 second cycle would require a 15 liter tank.

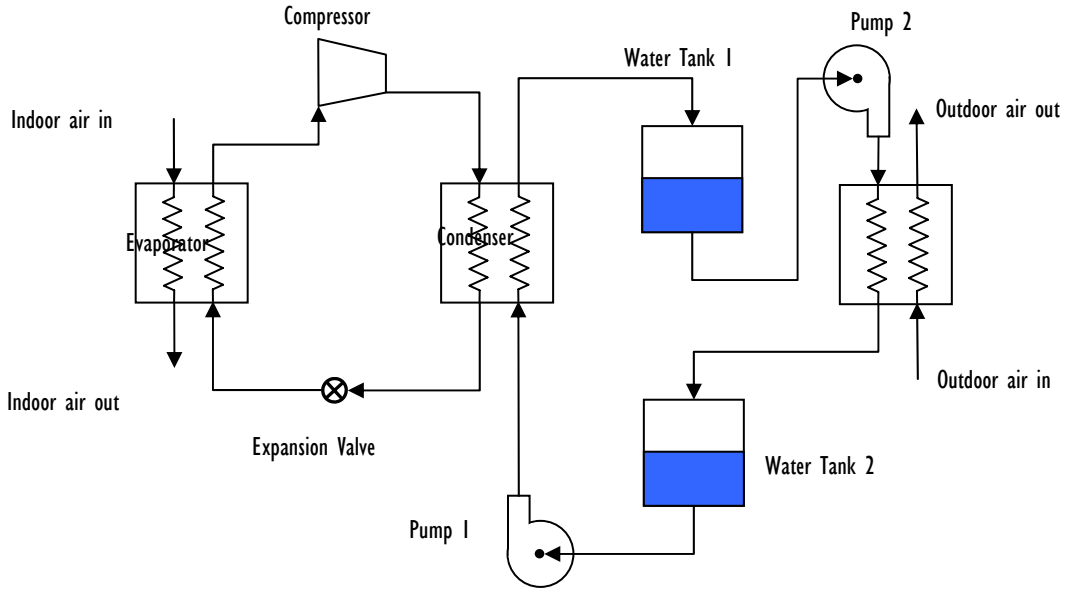

Figure F.2 Diagram of a secondary water loop with storage tanks

During the on cycle, hot water accumulates in water tank 1 as pump 1 operates at a higher flow rate than pump 2, which is then used during the off cycle.

Table F.1 shows calculations at different operating conditions using a simple LMTD model, where both heat exchangers have a maximum 1 degree approach difference at their maximum load conditions. The condenser requires the greatest UA at its lowest [say 0.3] runtime fraction because its water flow rate is maximum there, while the outdoor coil's UA sees maximum load at full speed conditions. Had the condenser been sized for the full load condition, its potential energy savings would have been diminished by the ~3x greater LMTD at that condition.

Table F.1 Condensing temperatures

			Cycling Chiller	VS chiller	VS (no loop)
Q_{cond} [KW]	T_{amb} [°C]	T_{water} [°C]	$T_{cond\ ON}$ [°C]	T_{cond} [°C]	T_{cond} [°C]
1	35	36 - 44	44.1	44.1	43
0.5	27	27.5 – 31.5	32.1	31.6	31
0.3	23	23.3 - 25.7	26.7	25.7	25.4

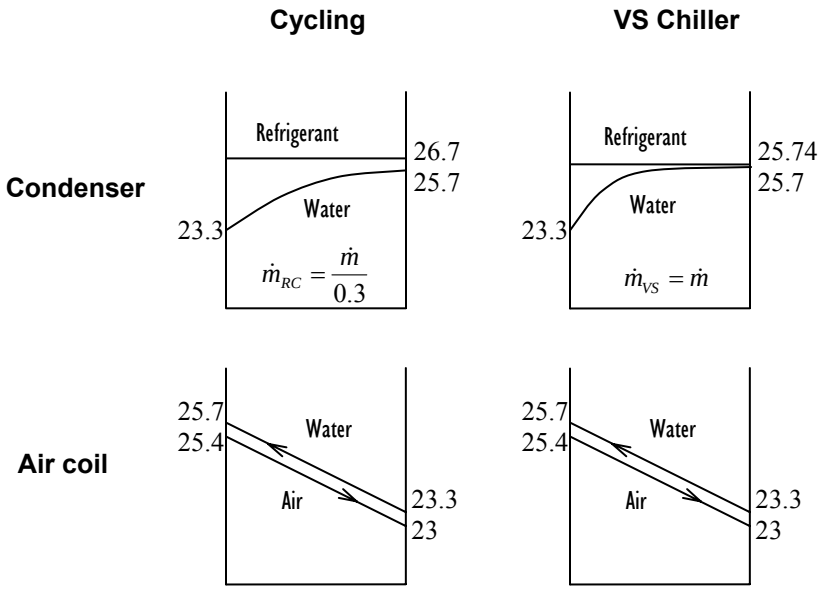

Figure F.3 Approach temperatures of 0.3 KW water loop systems with the same heat exchangers.

Table F.1 shows that the VS direct-expansion system would have the lowest condensing temperature at the full-load operating condition, because it has no secondary loop that imposes a 1°C approach temperature difference. Both the cycling and variable-speed secondary loop systems suffer from this penalty. At low load conditions the condensing temperature of the variable speed chiller system approaches that of the variable speed direct-expansion system (with no water loop) because the LMTD diminishes for low loads. While the cycling system with water storage tanks has the same condensing temperature as the variable speed chiller at full speed (the tanks are not used), at low loads, its condensing temperatures during its on cycle are larger than the VS chiller because of the temperature lift penalty associated with heating a greater amount of water ($1/\mu$). Recall that it also sustains similar lift penalties on the low side of the system (1°C due to the extra heat exchanger, plus the increased refrigerant pressure drop and temperature difference in the evaporator inherent to rapid cycling.

Because of the temperature lift penalties at the two extra heat exchangers, the cycling chiller system with the single-speed compressor will always be less efficient than the VS direct-expansion system, because its water pumping losses are the same order of magnitude as the VS system's inverter losses. However this disadvantage might be partially offset by the dissipative portion of the startup power spikes in the rapid cycling direct-expansion system. In the cycling chiller system these dissipative losses are negligible because the extra thermal capacitance provided by the water loop extends the cycle period so much that the spike duration is negligible.

Table F.2 provides a broader overview of the losses and limitations of a rapid cycling and variable speed system and their counterparts with water loops. Note that the VS chiller option is the least efficient. It is also apparent that the extra costs of the water loop for the cycling chiller, and its inherent inefficiency, means that it is unlikely to displace the VS or RC direct expansion systems. So long as the reliability risks associated with the RC system do not offset its inherent cost advantage over the inverter-driven system, it may offer a competitive alternative to VS systems. Future analyses should focus on the details of these two systems, since it appears

infeasible to substantially extend cycle lengths either by adding metal or water mass to the evaporator and condenser.

Table F.2 Simplified comparison of losses and limitations

	Losses	Limitations
RC	ΔT_{ref}, ΔP penalties Air duct losses	Cycle lengths (thermal mass) Power spikes
VS	~5% inverter Air duct losses ~5% pumping	Inverter Cost
Cycling chiller	Extra heat exchanger ΔT ΔT_{ref}, ΔP penalties	Loop, tank, pump costs
VS chiller	~5% inverter ~5% pumping Extra heat exchanger ΔT	Inverter and loop cost

At off design conditions on the low side of the system, the evaporator temperature cannot be increased due to the dehumidification requirements. The efficiency benefit in this case is therefore not achieved by reducing lift, but is realized as reduced water pumping power. While the water temperature glide is still the same as at full speed, at off design conditions the pumping power is reduced proportional to the reduction in water flow rate through the air coil. Limitations of lift savings on the low side of the system due to the dehumidification requirements are inherent to capacity modulation and are similar for all variable speed and rapid cycling systems.

Appendix G: Components for low side design.

In the low side of the system with a microchannel evaporator, different components could be used to improve performance of the system. There were three main goals that needed to be achieved by the setup of the components.

- The compressor inlet had to be superheated at all times to prevent damage to the compressor.
- The use of the evaporator had to be optimized to prevent dryout which would degrade performance.
- During the off-cycle, the performance of the system had to be maximized.
- A liquid condition must be maintained at the expansion valve to prevent choked flow.

There are two benefits to keeping the evaporator as saturated as possible during the on cycle. One is that with a larger liquid inventory in the evaporator, more cooling can take place during the off cycle (more liquid can boil). Also the high quality region of the evaporator has higher heat transfer resistance. To achieve these goals there are a number of different combinations of components that could be used.

G.1 High side receiver

The addition of a high side receiver had the advantage of being able to utilize the condenser more effectively even when it was not oversized as in the 1-ton evaporator experiments. In essence the high side receiver allowed us to ensure that experiments were not affected by an over or under charged system across the range of operating conditions.

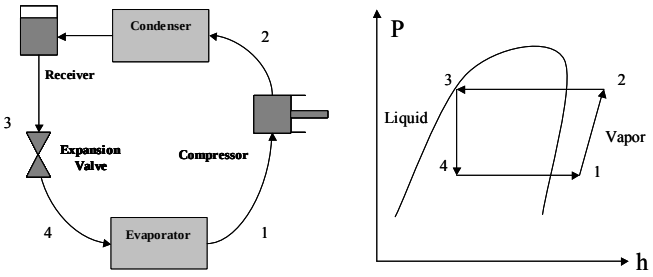

Figure G.1.1 Schematic and thermodynamic cycle with a high side receiver. (Uribe)

In addition, the high side receiver had the advantage of supplying saturated liquid to the expansion valve, preventing bubbles that could delay rapid re-establishment of the liquid inventory in the evaporator. The only real drawbacks of the high side receiver were its cost, and that systems cannot have more than one receiver at a time. Most of our experiments were run with a high side receiver, but further experiments might show its absence to have little adverse impact on system performance.

G.2 Suction Line Heat Exchanger

In order to make the most efficient use of the evaporator, a suction line heat exchanger was considered. Conventional advantages of a suction line heat exchanger are that it superheats the saturated evaporator exit and that it prevents bubbles in the expansion valve. The additional benefits of a high-efficiency suction line heat exchanger were that the inlet quality could be reduced to around 1%, creating better distribution in the evaporator, and that we

were able to keep a larger liquid inventory in the evaporator due to the fact that the exit is kept saturated. However it was found that our high efficiency suction line heat exchanger also made it susceptible to condensation on the vapor (low) side during the off cycle, which heated the liquid line and increased in the quality of the refrigerant going into the evaporator. While not significantly affecting system performance in our system due to the small amount of condensation, care must be taken to account for this effect in design of systems for rapid cycling.

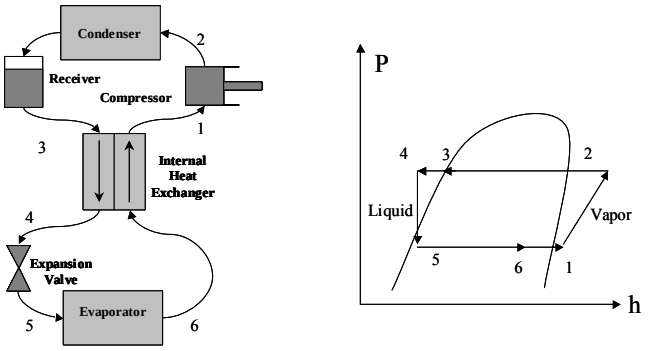

Figure G.2.1 Schematic and thermodynamic cycle with a suction line heat exchanger and a high side receiver. (Uribe)

Since the suction line heat exchanger is very efficient, the evaporator exit quality during steady state operation can be kept as low as 80% as opposed to a superheated condition, this increased the liquid inventory in the evaporator by about 80% directly increasing its off cycle cooling capacity. In most of our experiments a high effectiveness suction line heat exchanger was used. Experiments were also performed with a lower effectiveness (smaller) suction line heat exchanger to observe the effects of a smaller low side volume. The experiments with suction-liquid heat exchange showed a dramatic decrease in performance presumably because refrigerant maldistribution and the presence of a superheated region (to protect the compressor) in the evaporator overwhelmed the positive effect of reducing dryout by allowing the rapid increase in off-cycle saturation pressure to terminate boiling in the evaporator.

G.3 Low Side Receiver

A low side receiver would not work well with a rapid cycling system because it provides only part of the benefits a suction line heat exchanger would. A low side receiver would be placed after the evaporator, maintaining a saturated vapor evaporator outlet condition. In such a configuration the valve could be used to control condenser sub cooling.

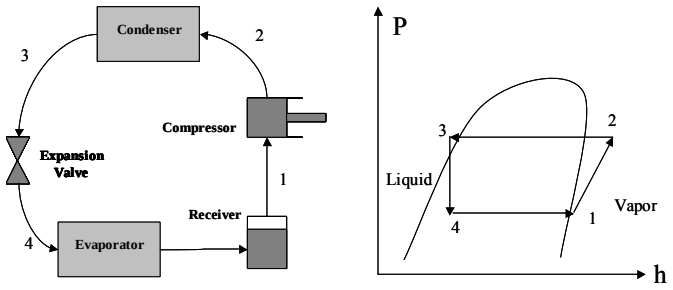

Figure G.3.1 Schematic and thermodynamic cycle with a low side receiver. (Uribe)

A large receiver on the low side would increase the low side volume and provide a cold sink for vapor coming from the evaporator during the off cycle. While this is not necessarily bad, its level needs to be carefully managed to prevent quick dryout of the evaporator.

G.4 Flood Tank

Theoretically a flood tank could be the simplest solution to the problems presented by the rapid cycling system. It would allow pure liquid going into the evaporator in addition to a saturated exit condition using only one component.

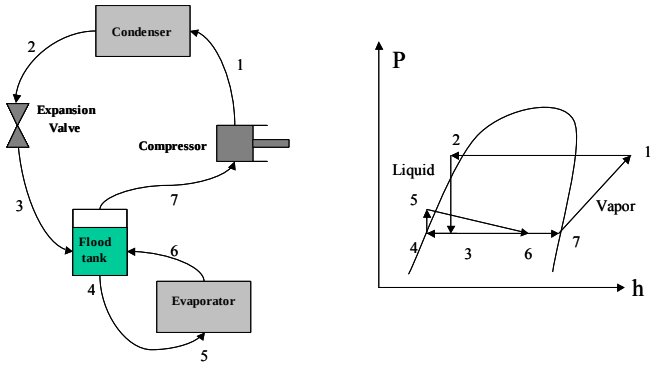

Figure G.4.1 Schematic and thermodynamic cycle with a flood tank. (Uribe)

In practice, however, a flood tank would not have worked in our lab because of the excessive head pressure required in the evaporator during steady state (on-cycle) operation. The maximum steady state pressure drop in our evaporator was approximately 60 kPa at full speed operation which corresponds to approximately 5m of R22 head pressure. In our lab it was not practical to create 5m of head pressure, hence flood tank tests were not performed. Even though the pressure drop in our evaporator was excessive due to the heat exchanger being designed as a CO2 gas cooler, a better designed evaporator would still need significant head pressure to flood the evaporator exit during the off-cycle. Another concern that would have to be addressed with the use of a flood tank is assuring oil return to the compressor. Also, the flood tank alone does not ensure a liquid condition going into the expansion valve, so it would have to be used with a suction line heat exchanger with the expansion device controlling compressor suction superheat.

G.5 Flash Gas Bypass

Another component for optimization of the low side that was considered was a flash gas bypass. This component works similar to a flood tank and does not have the head pressure problem; however it does not by itself provide a way for the evaporator exit to remain saturated.

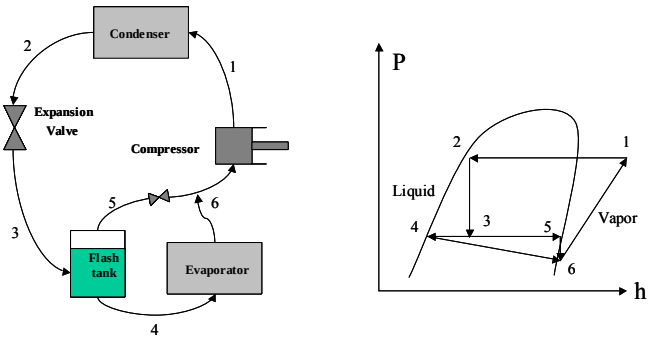

Figure G.5.1 Schematic and thermodynamic cycle with a flash gas bypass. (Uribe)

For maximum performance the flash gas bypass was tested with a suction line heat exchanger. In actual experiments the performance was found to be sub-optimal due to quick dryout of the evaporator, presumably due to condensation in the flash tank or the suction line heat exchanger with a small liquid inventory in the evaporator. Another drawback is the difficulty controlling the level in the flash tank under rapid cycling conditions, and that it is incompatible with a high side receiver.

With a flash gas bypass, other alterations could be made to enhance off-cycle performance of the system. For instance a check valve could be installed at the evaporator inlet so that during the off-cycle liquid is able to move into the evaporator more quickly.

G.6 Recommended Configuration

From our experiments and through careful consideration the optimal configuration for our system is a system with a high side receiver and a suction line heat exchanger. This allows for the best possible off-cycle performance of the system. The expansion valve will always have liquid going through it and the suction line heat exchanger ensures that quality is very low. In addition, the evaporator outlet can have quality <1, which increases the cooling capacity of the evaporator during the on cycle because no part of the evaporator is dried out and during the off cycle because there is a larger liquid inventory.

However, theoretically the optimal solution for a rapid cycling system with a microchannel heat exchanger would be to use a combination of a flash gas bypass and a suction line heat exchanger. This would accomplish all the goals and be a better option than the high side receiver and suction line heat exchanger combination because pure liquid would be entering the evaporator instead of ~1% quality and during the off cycle more liquid would drain into the evaporator. During the off cycle this systems benefits would especially be realized. Careful management of the liquid level in the flash tank would allow a precise amount of boiling to occur in the evaporator until the refrigerant to metal temperature difference is reduced to zero. A typical, 2 liter low side vapor volume allowed ~5 g of liquid to be boiled to close a 3 degree temperature difference between the refrigerant an the metal. However with a flash tank this temperature difference cannot be closed before the temperature of the entire thermal mass of liquid refrigerant also rises 3 degrees. About 10 g of condensation would occur in a flash tank holding 500g before enough energy has been passed to it to raise its temperature. The total refrigerant boiled can therefore be managed by the level in the flash tank. The amount of low side boiling would be designed so that boiling stopped before the evaporator dried out, using the thermal mass of the heat exchanger to extend the cycle further. In our lab

facility we tested a FGB and were able to conclude that it prevents maldistribution. However, a definite test was not possible as we were not able to put the flash tank above the evaporator so the vapor produced by off-cycle boiling could return via the bypass line to the flash tank where it would re-condense. The location of the FGB also did not allow for off-cycle drainage into the evaporator.